UNIVERSITÀ
DEGLI STUDI
DI PADOVA

Sede Amministrativa: Università degli Studi di Padova

Dipartimento di PEDIATRIA “SALUS PUERI”

SCUOLA DI DOTTORATO DI RICERCA IN: *MEDICINA DELLO SVILUPPO E SCIENZE DELLA PROGRAMMAZIONE*

INDIRIZZO: *MALATTIE RARE, GENETICA, BIOLOGIA E BIOCHIMICA*

CICLO XXIV

ADMINISTRATION OF L-CITRULLINE IN AN ANIMAL MODEL OF PERINATAL LUNG DAMAGE

Direttore della Scuola : Ch.mo Prof. Giuseppe Basso

Coordinatore d’indirizzo: Ch.mo Prof. Giorgio Perilongo

Supervisore :Ch.mo Prof. Lino Chiandetti

Dottorando : Dott. Arben Dedja

INDEX

Riassunto

La corioamnionite indotta dalla somministrazione intrauterina dell'endotossina LPS e da una moderata iperossia nei primi giorni di vita causano uno squilibrio alveolare e vascolare del polmone nel ratto neonato. L'ossido nitrico (NO) endogeno, che promuove la crescita polmonare, viene prodotto nelle cellule endoteliali dal metabolismo del L-arginina verso il suo prodotto, la L-citrullina. Abbiamo studiato l'efficacia della somministrazione di L-citrullina in un modello di danno indotto da corioamnionite e/o da iperossia nei ratti neonati nell'attenuare il danno polmonare intervenendo sulla sintesi del NO endogeno aumentando i livelli di L-arginina.

***Materiali e Metodi*.** I ratti neonati (che ricevono o no LPS nella loro fase intrauterina) vengono esposti a un FiO2=0.6, o ad aria ambiente, per 14 giorni dopo la nascita con la somministrazione, per alcuni di loro, della L-citrullina. A vari *time-points* sperimentali siero e tessuto polmonare vengono raccolti per ulteriori analisi. Le sezioni polmonari vengono colorate con ematossilina & eosina e fotografate a 10X. Per una valutazione della densità vascolare le sezioni sono colorate per la presenza dell'antigene del Fattore di von Willebrand. La VEGF e l'espressione proteica eNOS vengono esaminati con il Western blot. La HPLC Spettrometria di Massa viene usata per determinare e quantificare nel siero ADMA, SDMA, L-arginina, L-citrullina, NMMA e omo-arginina.

***Risultati*.** L'esposizione a moderati regimi di iperossia era associata istologicamente con aree estese di tipo enfisematoso, simile al quadro del gruppo esposto al LPS e, inoltre, con un arresto dell'alveolarizzazione e contestuale variazione eterogenea della morfologia polmonare, e ha indotto un cambiamento nella morfometria polmonare con aree irregolari di inspessimento parenchimatoso intervallate da aree con spazi aumentati. Il gruppo ricevente il farmaco presentava un grado di alveolarizzazione più sviluppata con un incremento del numero degli alveoli per mm^2, statisticamente significativo rispetto al gruppo con iperossia. Le sezioni polmonari dei gruppi CITR+iperossia e LPS+CITR contenevano spazi più piccoli e più numerosi, simili ai controlli. Il numero delle creste secondarie era più alto nei controlli e nei gruppi CITR+iperossia e LPS+CITR, che nei gruppi con iperossia solo, o LPS sola. L'espressione genica del VEGF era più bassa nel gruppo dell'iperossia, rispetto al gruppo CITR+iperossia, o ai controlli. Inoltre, le sezioni polmonari da animali di controllo o da trattati con CITR+iperossia presentavano un'espressione vWF simile, mentre la colorazione era più bassa nel gruppo con iperossia. Nei campioni da animali trattati con CITR+iperossia era evidente anche un organizzazione migliore della rete vascolare rispetto agli animali esposti solo all'iperossia. La quantità delle proteine eNOS normalizzate nei tessuti polmonari da animali trattati con L-citrullina era più alta che nei

tessuti del gruppo con sola iperossia. La valutazione con spettrometria di massa dei campioni di siero non ha mostrato grandi differenze tra i gruppi trattati.

***Conclusioni*.** In conclusione abbiamo provato che: (i) la somministrazione della L-citrullina aiuta la crescita alveolare nel danno polmonare da ossigeno, o da esposizione antenatale a endotossina; (ii) il gene e la proteina VEGF sono over-espressi nel gruppo trattato con L-citrullina. Ulteriori effetti protettivi potranno essere manifesti sul network alveolare e vascolare del polmone e, di conseguenza, sulla maturazione della matrice nel nostro modello di danno polmonare; tutto questo potrà essere promettente in vista di una strategia della prevenzione della broncodisplasia polmonare.

Abstract

Moderate hyperoxia and induced chorioamnionitis by intrauterine administration of endotoxin LPS into near-term pregnant rats cause alveolar and vascular lung derangement in the newborns. Endogenous nitric oxide (NO), which promotes lung growth, is produced from the metabolism of L-arginine to L-citrulline in endothelial cells. We investigated whether administering L-citrulline by raising the serum levels of L-arginine and enhancing NO endogenous synthesis, attenuates lung injury in a chorioamnionitis and/or moderate hyperoxia-induced model. ***Material and Methods*.** Newborn rats (receiving or not intrauterine LPS) were exposed to FiO2=0.6 or room air till 14 days after birth and were administered L-citrulline. Serum and lung tissues were collected for further analysis. The lung sections were subsequently stained with H&E and photomicrographs were obtained at 10X magnification. For vessel density assessment, sections were stained to reveal the presence of von Willebrand Factor Antigen. VEGF and eNOS protein expression was examined by Western blot. High performance liquid chromatography-mass spectrometry was used for simultaneous determination and quantification of ADMA, SDMA, L-arginine, L-citrulline, NMMA and homo-arginine in the serum. ***Results*.** The lung histopathology analysis of the Hyperoxia group showed a pattern typically emphysematous, similar to the LPS exposure group, when compared to controls. Exposure to hyperoxia was associated with an arrested alveolarization, inducing a change in lung morphology with patchy areas of parenchymal thickening interspersed with areas of enlarged air spaces. The lung sections of the CITR+hyperoxia and LPS+CITR rats contained smaller and more numerous air spaces, and were more similar to the control lungs. The mean alveolar size was higher in Hyperoxia group *vs.* controls, or LPS+CITR, in a *post hoc* comparison unchanged with respect to CITR+hyperoxia, or LPS, or CITR. The secondary crests were higher in the Control and CITR+hyperoxia and LPS+CITR groups than in the Hyperoxia only, or LPS only groups. VEGF gene expression evaluated by real-time quantitative PCR was lower in the Hyperoxia group, than in the CITR+hyperoxia or Control groups. Also, lung sections from Control and CITR+hyperoxia animals showed a similar vWF expression, whereas staining was weaker in the Hyperoxia group. In the CITR+hyperoxia sections there was also evidence of a better organization of the vessel network than in animals exposed to hyperoxia. The amount of eNOS protein normalized in the lung tissue from the L-citrulline treated animals was higher than in the tissues from the Hyperoxia group. Serum assessment with mass spectrometry did not show major differences in the time course and treatment groups. ***Conclusions*.** Our main findings were that: (i) administering L-citrulline proved effective in improving alveolar growth after oxygen-induced and

antenatal endotoxin exposure lung damage; (ii) VEGF gene and protein were over-expressed in the group treated with L-citrulline. There may have been further protective effects on the alveolar vascular network and, consequently, on matrix maturation in our model and this may be promising with a view to BPD prevention strategies.

Abbreviations

ADMA = Asymmetric dimethylarginine

ARG = L-arginine

BPD = Brochopulmonary dysplasia

BSA = Bovine Serum Albumine

CITR = L-citrulline

DAB = Diaminobenzidine

DDAH = Dimethylarginine dimethylaminohydrolase

eNOS = endothelial Nitric Oxide Synthase

FiO2 = Fraction of inspired Oxygen

GAPDH = Glyceraldehyde 3-phosphate dehydrogenase

hpf = high-powered field

HPLC/MS = high performance liquid chromatography-mass spectrometry

IPAH = Idiopathic Pulmonary Arterial Hypertension

iNOS = inducible Nitric Oxide Synthase

i.u. = intrauterine

LPS = Lipopolysaccharides

MLI = mean linear intercept

MRM = Multiple reaction monitoring

NMMA = N^G-monomethyl-L-arginine

nNOS = neuronal Nitric Oxide Synthase

NO = Nitric Oxyde

P = Postnatal

PBS = Phosphate buffered saline

PRMTs = Protein arginine methyl-transferases

PVDF = polyvinyl difluoride

RDS = Respiratory Distress Syndrome

rpm = revolutions per minute

SDMA = Symmetric dimethylarginine

SDS-PAGE = Sodium Dodecyl Sulphate – PolyAcrylamide Gel Electrophoresis

SE = Standard error

TBS = Trisbuffered saline

VEGF = Vascular endothelial growth factor

vWF = von Willebrand Factor Antigen

Introduction

Lung development

Human lungs are alveolated at birth and alveolarization starts at the beginning of the saccular phase of lung development with the appearance of secondary crests at 28 weeks of gestation. Typical alveoli are readily apparent at 36 weeks of gestation in all human fetuses and other observers have recognized alveoli even earlier.

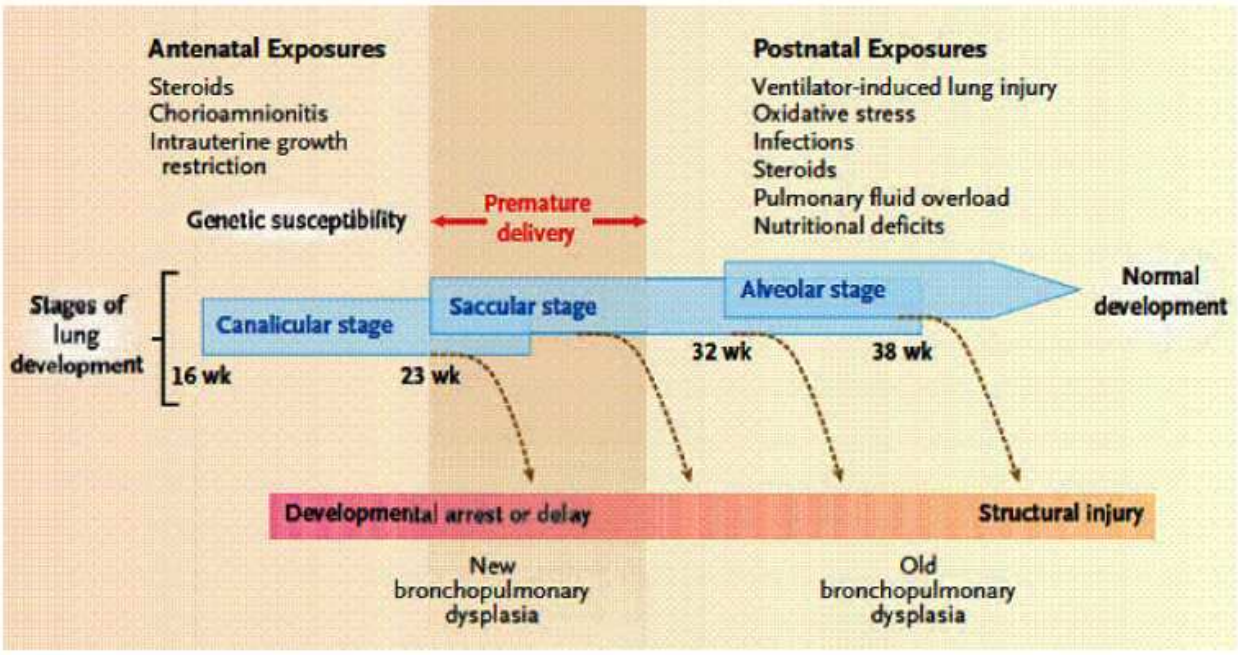

Fig. 1 Stages of lung development, potentially damaging factors and types of lung injury. *(from: Baraldi E & Filippone M. N Engl J Med, 2007)*

In premature newborns, the lungs are often exposed to several sources of injury, before and after birth. Such exposures, as well as genetic susceptibility to problematic lung development, may cause direct airway and parenchymal damage, inducing a deviation from the normal developmental path. Depending on the timing and extent of the exposures, lung injury may range from early developmental arrest to structural damage

of a relatively immature lung (new & old brochopulmonary dysplasia). Premature infants born at a gestational age of 23 to 30 weeks – during the canalicular and saccular stages of lung development – are at the greatest risk for bronchopulmonary dysplasia.

Chorioamnionitis – a multiorgan disease of the fetus

Despite technological and therapeutic advances in the past few years, premature birth continues to be a worldwide major health problem. In the West World, the incidence of this phenomenon varies between 5 and 13% of all the live births (Goldenberg *et al*, 2008). Roughly, the causes of preterm birth can be divided into two groups: indicated preterm birth and preterm birth preceded by spontaneous preterm labor or preterm pre-labor rupture of the membranes (Goldenberg *et al*, 2000). The latter group is often associated with intrauterine inflammation or chorioamnionitis (Goldenberg *et al*, 2008 e 2000). A close association between chorioamnionitis and spontaneous preterm delivery exists (Goldenberg *et al*, 2000). As a result, the proportion of preterm infants exposed to chorioamnionitis increases with decreasing gestational age up to 80% below 28 weeks of gestation (Lahra *et al*, 2009; Lahra *et al*, 2008). Ascending bacterial invasion of the uterine cavity is thought to be the most common route of infection, although bacteria are identified only in the minority of cases (Goldenberg *et al*, 2000). Bacteria secret the endotoxin lipopolysaccharide (LPS), a glycolipid present in the outer membrane of gram-negative bacteria that is composed of a polar lipid head group (lipid A) and a chain of repeating disaccharides (Raetz *et al*, 1991). Most of the biological effects of LPS are reproduced by lipid A (Schromm *et al*, 2000), although the presence or absence of the repeating oligosaccharide O antigen influences the magnitude of the response (Kelly *et al*, 1991). Changes in the lungs become evident within 2–4 h and include hypoxemia with an increase in the alveolar-arterial oxygen difference (Matute-Bello *et al*, 2008). Nevertheless, a large subset of chorioamnionitis cases remain clinically silent. These may be diagnosed by culture or proteomic profiling

of the amniotic fluid, by microbial culture or foot-printing, or by histological examination of the placenta after birth. The latter is generally regarded as the 'gold standard' in the diagnosis of chorioamnionitis (Faye-Petersen, 2008). More serious cases of chorioamnionitis may become clinically apparent and cause both general (fever, leukocytosis and raised C-reactive protein) and local symptoms (uterine tenderness and vaginal discharge). Although a combination of these symptoms is often given the description 'clinical chorioamnionitis', the overlap with the histological diagnosis of chorioamnionitis has been shown to be only modest (Been *et al*, 2009). When intrauterine inflammation is present, the fetus may be exposed through direct contact with amniotic fluid or through the placental–fetal circulation. Thus, chorioamnionitis is implied in the pathogenesis of BPD, as well as in premature births and, consequently, in mechanical trauma related to ventilation and toxicity due to oxygen use (Yoon *et al*, 1999; Speer, 2003). Functional or parenchyma injured alveolar-capillary barrier leads to early Respiratory Distress Syndrome (RDS), even quickly resolved, nevertheless a rise in BPD is known (Watterberg *et al*, 1996). Fetus under chorioamnionitis presents multiorgan failure especially in brain and lung. Clinical chorioamnionitis was shown to be associated with an increased risk for RDS whereas a short-term beneficial effect on incidence and severity of RDS could be demonstrated for histological chorioamnionitis. Also, existing data support a role of chorioamnionitis for cystic periventricular leukomalacia, cerebral palsy and intraventricular hemorrhage in preterm infants (Thomas *et al*, 2011). Regarding our organ of interest, the lung, preterm birth is highly associated with respiratory distress syndrome (RDS), caused by structural and functional immaturity of the newborn lung. A modulating role of intrauterine exposure on lung immaturity has been recognized for many years (Been *et al*, 2009). Watterberg *et al* were the first to show an ambivalent association between chorioamnionitis and respiratory morbidity. In ventilated preterm infants they were able to show a decrease in RDS, but a subsequent increase in

chronic lung injury (BPD) after chorioamnionitis. Many studies since then have reproduced the association between intrauterine inflammation and decreased RDS incidence, as reviewed recently (Been *et al*, 2009). Despite a reduction in acute respiratory problems, several early human studies have shown chorioamnionitis to be associated with a paradoxical increase in chronic lung disease of prematurity (Been *et al*, 2009; Watterberg *et al*, 1996). The molecular mechanisms and the clinical implications are just beginning to be studied and understood.

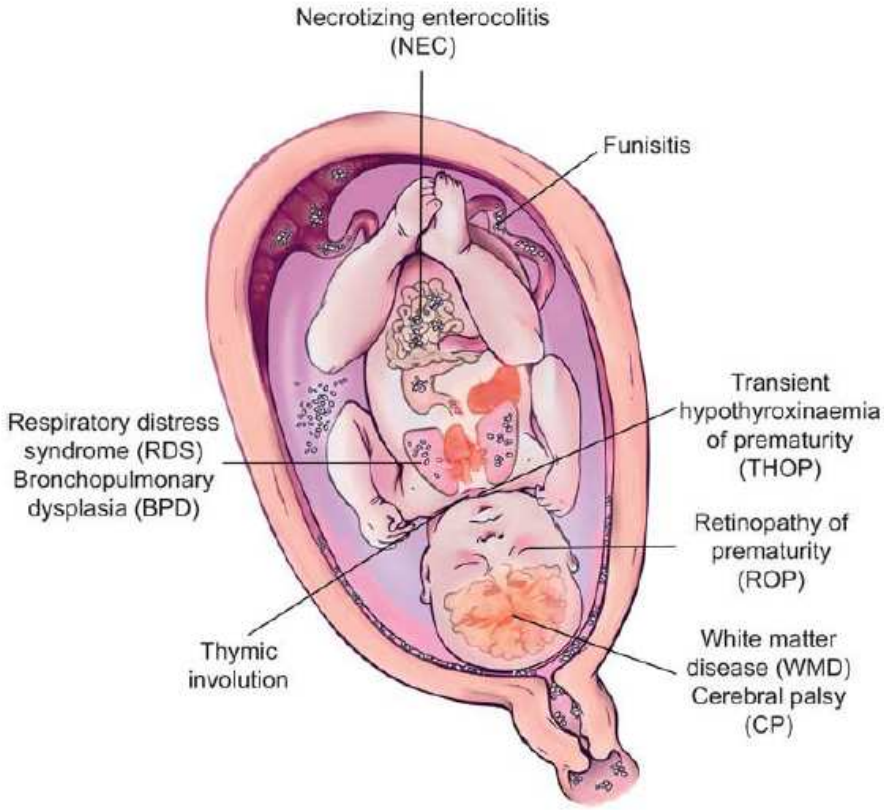

Fig. 2. Chorioamnionitis, as a multiorgan disease of the fetus. The fetus is being exposed to contaminated amniotic fluid that is aspirated and/or slicked by the fetus *(from: Gantert M et al. J Perinatol, 2010)*.

Nitric Oxide

Mammalian nitric oxide (NO) synthesis is catalyzed by three isoforms of nitric oxide synthase (NOS) that have different tissue distributions: neuronal NOS (nNOS), endothelial NOS (eNOS) and inducible NOS (iNOS). L-arginine is the substrate for all three isoforms of NOS. Following their incorporation into proteins, L-arginine residues that lie within certain sequences can be methylated by protein arginine methyltransferases. Proteolysis of arginine-methylated proteins releases free methylarginines into the cytosol. Asymmetrically methylated arginines are the only product of post-translational protein modification known to exert substantial biological effects. Asymmetric methylarginines are competitive inhibitors of NOS enzymes; they compete with L-arginine to bind to the active site of

NOS. The post-translational modification and subsequent proteolysis of these modified proteins releases free methylarginine residues into the cytosol; from here, these residues can pass out of the cell into the plasma.

Three forms of methylated arginine – which can be considered arginine analogues – have been identified in eukaryotes: N^G-monomethyl-L-arginine (NMMA); ADMA; and ω-N^G,N'^G-symmetric dimethylarginine (SDMA) (Kakimoto & Akazawa, 1970). The asymmetric methylarginines – NMMA and ADMA – are inhibitors of the NOS family of enzymes. All three methylated arginines (ADMA, NMMA and SDMA) are inhibitors of arginine transport at super-physiological concentrations, although the physiological relevance of this inhibition remains unclear (Closs *et al*, 1997; Tsikas *et al*, 2000).

Circulating ADMA is present at higher concentrations than NMMA and is often considered to be the principal inhibitor of NOS activity (Vallance P, 1992). However, it is important to note that the relative concentrations of ADMA and NMMA may differ between tissues and organ systems and hence the contribution of endogenously produced NMMA to NO bioavailability may be of more importance in certain tissues.

ADMA is eliminated from the body by a combination of renal excretion and metabolism by the dimethylarginine dimethylaminohydrolase (DDAH) enzymes. This enzymatic pathway is therefore a potential endogenous mechanism for the regulation of NO production by competitive inhibition. ADMA is synthesized following the methylation of arginine residues in proteins by a group of methyltransferases that are termed protein arginine methyl-transferases (PRMTs) (Paik & Kim, 1967; Katz *et al*, 2003). Methylarginines only appear in the cytosol as a result of protein degradation, and no direct synthetic route for the production of ADMA, SDMA and NMMA from free arginine has yet been identified. Furthermore, the synthesis and degradation of methylated arginines are closely coupled with the synthesis and degradation of methylated proteins (Miyake & Kakimoto, 1976). Thus, intracellular ADMA levels appear to be governed

by PRMT activity, protein turnover and clearance. Although it was originally assumed that renal excretion was the sole route of clearance for free methylarginines, metabolic studies have identified a catabolic pathway for NMMA and ADMA (Kakimoto. & Akazawa, 1970).

Two catabolic pathways have now been identified for methylarginines. The first pathway, which is catalysed by DDAH, is specific for asymmetric methylarginines and accounts for >80% of their *in vivo* metabolism (Ogawa *et al*, 1987). The second minor pathway utilizes both asymmetric and symmetric methylated arginines as substrates, and is catalysed by alanine-glycoxylate aminotransferase (AGXT2) (Ogawa *et al*, 1990). The significance of DDAH-catalysed methylarginine metabolism has been calculated using estimates of daily protein turnover and protein methylarginine content (Vallance *et al*, 1992) in human urine and plasma. Based on these values, it has been predicted that if active metabolism did not occur, there would be a daily increase in plasma ADMA concentrations of approximately 5 μM per L (Achan *et al*, 2003). These levels greatly exceed the *Ki* of ADMA on NOS, and such accumulation would result in substantial inhibition of NOS signaling *in vivo*. In the vast majority of various diseases that link ADMA, there is an association between increased plasma ADMA concentrations and disease pathology. Furthermore, the increased levels of ADMA in the development and progression of cardiovascular diseases has been postulated to be related to the ADMA-mediated inhibition of eNOS activity. Consistent with the hypothesis that DDAH regulates ADMA levels and NO signaling *in vivo*, studies that were carried out in animal models and humans have demonstrated changes in DDAH expression and/or activity in disease states in which impaired NO signaling has been implicated in pathophysiology.

In children with congenital heart disease, ADMA levels were significantly increased in patients who displayed mean pulmonary arterial pressures that were >25mm Hg (Gorenflo *et al*, 2001). No significant change in

ADMA levels was observed in patients who displayed high pulmonary flow but normal pulmonary pressures. These data suggest that increased ADMA concentration may play a part in the elevation of pulmonary vascular resistance in these patients. Similarly, there is an increase in both ADMA and SDMA in plasma taken from patients with idiopathic pulmonary arterial hypertension (Pullamsetti *et al*, 2005). Moreover, in lung tissue biopsies taken from patients with idiopathic pulmonary arterial hypertension, levels of intracellular ADMA and SDMA were increased, whereas mRNA and protein levels of DDAH2 were significantly reduced. NO is also known to have pro-angiogenic effects (Cooke, 2003), thus inhibition of NO could be beneficial for limiting tumour angiogenesis and growth. Maternal endothelial dysfunction is observed in pre-eclampsia and there is increasing evidence showing that elevated ADMA levels may contribute to the pathological features observed in this disorder (Speer *et al*, 2008), although in some studies this association is not apparent (Kim *et al*, 2006). The ADMA-DDAH-NOS pathway has not yet been ultimately studied in the chorioamnionitis field, since an increase of early exhaled NO, or ADMA levels were found in preterm newborn infants (Alfiero-Bordigato *et al*, 2011; Figueras-Aloy *et al*, 2011).

Role of L-citrulline

Oral supplementation with L-arginine has been shown to enhance NO-mediated vasodilatation in several (Bode-Böger *et al*, 2003; Piatti *et al*, 2001), but not all clinical studies (Walker *et al*, 2001). L-arginine is unfortunately subject to extensive pre-systemic and systemic elimination, by bacteria in the gut and arginases in the gut and liver, respectively (Morris SM Jr., 2004), unlike the non-essential amino acid L-citrulline, which is converted into L-argininosuccinate by argininosuccinate synthase, and subsequently into L-arginine by argininosuccinate lyase (Curis *et al*, 2005). L-citrulline may therefore serve as an L-arginine precursor (Waugh *et al*, 2001) and many NO-producing cells (vascular endothelial cells and macrophages) use L-citrulline as a substrate to form L-arginine. Oral L-

citrulline supplementation raises plasma L-arginine concentrations and increases NO-dependent signaling in a dose-dependent manner (Schwedhelm *et al*, 2008). It has been shown that providing L-arginine to endothelial cells increases NO production, but only slightly by comparison with the much more marked increase induced by L-citrulline supplementation (Solomonson *et al*, 2003).

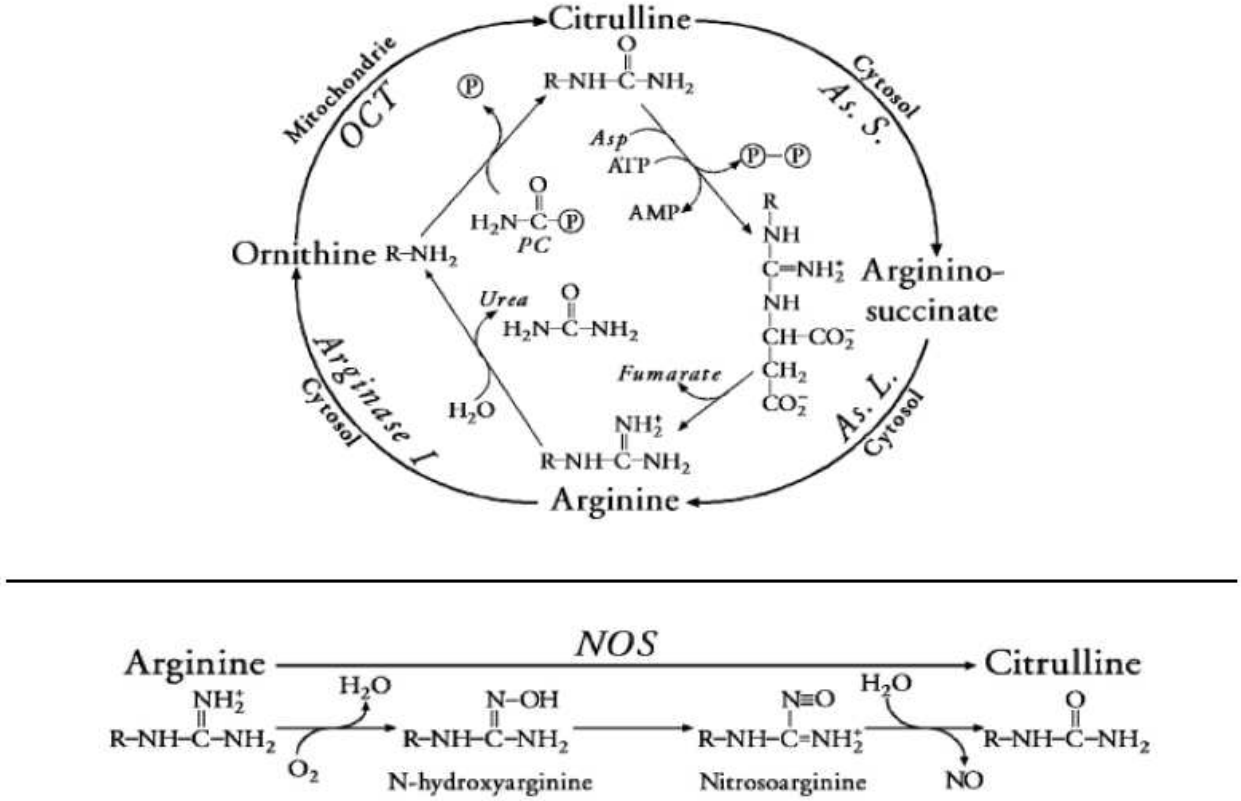

Fig. 3 The complexity of the urea cycle (top) and mechanism of the NO biosynthesis of the NO synthase (bottom). (*from: Curis E et al. Amino Acids, 2005*).

Aim of the study

Hypothesis

In the following study we analyzed the ADMA/Arginine/Citrulline pathway in a neonatal experimental set in rats, which translates the chorioamnionitis (with or without postnatal use of a moderate hyperoxia) and the related perinatal respiratory disease at birth. We have hypothesized that:

1) The antenatal fetal infection by endotoxin (LPS) causes substantial structural lung anomalies in the newborn rat – an experimental model "mimicing" chorioamnionitis;

2) Administering L-citrulline, and thereby raising serum levels of L-arginine, might attenuate lung damage induced by chorioamnionitis alone, or by chorioamnionitis combined with moderate hyperoxia, by raising the quota of endogenous NO, in an experimental model in the rat.

Primary objective

Verify the role of L-citrulline as a potential pre-clinic treatment of the chronic lung neonatal disease.

Secondary objectives

1) Verify the reliability of the pre-clinic model of chorioamnionitis in order to employ this model for further studies of perinatal lung damage;

2) Improve our knowledge about the impact of L-citrulline on endogenous NO metabolism in the neonatal lung disease caused by experimental chorioamnionitis, hyperoxia, or their combination.

Material and Methods

Animals

Female wild-type Sprague-Dawley rats and their offspring were housed and handled in accordance with the recommendations of the Public Health Office release of 17.12.2009, number 220/2009-B; law 116/92. The study was conducted on male or female rat pups kept together with their nursing mother in conventional facilities. The animals were fed *ad libitum* and exposed to alternating 12h day-night cycles.

Experimental design

Pregnant rats were preventively assigned randomly to give birth to pups that will enter the different experimental groups, schematized in the following figure.

Group	Trial	LPS *(10μg i.u.)*	Hyperoxia *(FiO2=0.60;CO2≤0.5%)*	CITR *(1g/kg/day i.p.)*
1 (n=14)	LPS + CITR	+	–	+
2 (n=24)	LPS	+	–	–
3 (n=18)	CITR+hyperoxia	–	+	+
4 (n=22)	Hyperoxia	–	+	–
5 (n=10)	LPS+hyperoxia+CITR	+	+	+
6 (n=8)	LPS+hyperoxia	+	+	–
7 (n=20)	Control	–	–	–
8 (n=24)	Control + CITR	–	–	+

Fig. 4 Experimental Design. LPS = rats receiving lipopolysaccharides; CITR = l-citrulline; Control = rats without LPS raised at room air

Along the normal development and maturation of the lung of the newborn rats, two main experimental time-points were set at 7 and 14 postnatal (P) days for each group. Moreover, we also set other two supplementary time-points at P3 and P10 for groups 1, 2, 7, and 8.

Animals assigned to groups 1; 2; 5 and 6 were injected with 10µg of intra-amniotic LPS (Escherichia coli 0111:B4; Chemicon International, USA), diluted in saline. Pups were let borne on term (22.5±0.5 days) by vaginal delivery. They received no supplemental oxygen or artificial ventilation at birth. Survival rate at birth was recorded. Pups assigned to groups 3 through 6 were placed under hyperoxia, along with their mothers, or foster mothers, within 30 minutes after birth in transparent, polished acrylic chambers where the oxygen concentration was maintained till 14 days at FiO2=0.60, by means of a software enabling continuous O2 and CO2 monitoring (BioSpherix, OxyCycler model A84XOV, Redfield, USA).

Also, for the experimental groups 1; 3; 5 and 8, L-citrulline ≥ 99.9% solution (Sigma, St. Louis, USA) dissolved in saline at a final concentration of 0.1mg/µl was administered subcutaneously once a day at a dose of 1g/kg.

Surgical technique for installation of chorioamnionitis

In order to inject intrauterine LPS, the surgical procedure was conducted in pregnant rats at the 20th day of the gestational age. Animals were delicately handled in general anesthesia, obtained with O2 administration with sevofluorane at 3-3.5% (induction) and with sevofluorane at 2% (maintenance) inhalation via face mask, potentiated with the analgesic tramadol.

After a 4cm long median inferior incision, the uterus with the fetuses was pulled out and was put over the abdomen in a gauze wet with warm saline. The total number of amniotic sacs in each mother rat was examined and recorded during laparotomy. The administration of LPS was quickly performed in the amniotic liquid of each fetus. The injection was done with a 30G needle in a Hamilton syringe for a volume of 10µl/per fetus (10µg of LPS). The uterus was then repositioned into the abdominal cavity. The

animal was closed in two layers and was let to wake up under a heating lamp.

Follow up

Pregnant rats were monitored closely to ensure arousal within 10 minutes after surgery. Afterwards, they were moved back to the cages and were monitored for activity, ability to drink and eat and for signs of bleeding or infection. After birth, groups 1; 3; 5; and 8 received L-citrulline ≥ 99.9% (Sigma, St. Louis, USA) administered subcutaneously once a day at the dosage of 1g/kg (with a concentration of 0.1mg/µl). Survival and body weight of the infant rats was monitored and recorded daily from birth throughout the study period. Survival rate was calculated as the number of survived pups divided by the number of sacs that received intra-amniotic injection in each given litter.

Tissue and fluid collection

At the experimental endpoint the animals were deeply anesthetized with a 1:1 combination of Zoletil (Zolazepam + Tiletamina) and xylazine and successively euthanized with Tanax®. Blood samples were centrifuged at 8000 rpm for 20 minutes at 4℃ and serum was then s eparated and stored at -80℃. The animals' trachea was cannulated and 4 % neutral buffered formalin was instilled at a pressure of 25 cmH2O during a 5 min equilibration period. The lungs were then removed and fixed overnight in buffered formalin, washed in PBS, serially dehydrated in increasing concentrations of ethanol and embedded in paraffin. The left lungs were excised, freeze-clamped in liquid nitrogen and stored at -80℃ for molecular studies.

Lung histopathologic analysis

Lung sections 4 µm thick were stained with hematoxylin and eosin. For each case, we examined six sections and three fields per section. Photomicrographs were obtained on a field of 568 µm x 422 µm at 10X magnification with a Leica DM 4000B microscope (Leica, Solms, Germany)

integrated with a camera (Leica DFC 280). Lung morphometric analyses were performed by two independent researchers blinded to the treatment strategy, using ImageJ, a public domain Java image-processing program created by Wayne Rasband at the Research Services Branch, National Institute of Mental Health, Bethesda, USA (http://rsb.info.nih.gov/ij). In particular, in each section from specific plug-in which leads to the evaluation of the skeletonized air spaces into each high-powerrd field (hpf), the averaged alveolar surface size was evaluated from considering the alveolar minimum and maximum diameter and excluding the areas of large airways or vessels from analysis. The intra-alveolar distance was measured as the mean linear intercept (MLI) by standard method, utilizing the same plug-in, by dividing the total length of lines drawn across the lung section (grid), by the number of intercepts encountered. A cell counter was applied for assessing the secondary crests number/hpf.

Vessel density

For vessel density assessment, 4 μm thick sections were stained to reveal the presence of von Willebrand Factor Antigen (vWF) with a rabbit polyclonal anti-vWF (Dako, Glostrup, Denmark; 1:8000 diluted). Specimens were then washed with PBS and incubated with Bond Intense R Detection Kit (Leica) according to the manufacturer's instructions. The staining was visualized with DAB and the slides were counterstained with hematoxylin. The sections were then dehydrated, cleared, and mounted. Formalin-fixed, paraffin-embedded normal lung was used as a positive control. Negative controls were obtained using an identical staining procedure and substituting the primary antibody with primary buffer.

For each case, we examined five sections and three fields per section. Images of vWF-related staining were obtained at 20X magnification with a Leica DM 4000B microscope (Leica, Solms, Germany) integrated with a camera (Leica DFC 280). The number of vWF-positive vessels (<100 μm in size) was counted per high-powered field.

VEGF and eNOS protein expression

VEGF and eNOS protein expression was examined by Western blot, as described elsewhere (Guidolin *et al*, 2008). Briefly, lung sections were homogenized with lysis buffer (0,6% TritonX-100; 0,15M NaCl; 10mM Tris pH 7.4; 1mM EDTA) containing protease and phosphatase inhibitors. Forty µl of protein lysate from whole cell lysate were denatured in loading buffer for 5 min, separated with SDS-PAGE gel, and transferred onto PVDF membranes. The blots were blocked for 1 h with 5% BSA in Trisbuffered saline (TBS), followed by incubation overnight with rabbit anti-VEGF (VEGF sc-507, Santa Cruz Biotechnology) at a dilution of 1:100, or mouse anti-eNOS/NOS Type III (BD Biosciences) at a dilution of 1:100. After washing with TBS, blots were incubated with a secondary antibody and visualized with ECL kits (Thermo Scientific). A mouse anti-human GAPDH protein antibody (Millipore) at a dilution of 1:1500 was used as a control for equal loading. The levels of protein were quantified by image analysis using the ImageJ software and densitometric data were expressed as the ratio of protein to GAPDH.

Mass spectrometric analyses

Serum ADMA, SDMA, L-arginine, L-citrulline, NMMA, and homo-arginine assessment were measured as stated elsewhere (Di Giangi *et al*, 2010). Briefly, L-citrulline, L-arginine, and N-methyl-L-arginine were purchased from Fluka (Sigma–Aldrich, St. Louis, USA); N^G,N^G-dimethyl-L-arginine hydrochloride, N^G,N^G-dimethyl-L-arginine, copper carbonate, cyanogen bromideactivated, dimethylamine, n-butanol and acetyl chloride were purchased from Sigma–Aldrich (St. Louis, USA). Isotope labeled internal standards: L-arginine-5-13C (99%, HPLC), 4-4,5,5-2H4 (95%, HPLC) and L-ornithine-3,3,4,4,5,5-2H6 (98%, HPLC) were purchased from Cambridge Isotope Laboratories (Andover, USA); L-citrulline-5,5-2H2 (99%, HPLC) was a generous gift from P. Rinaldo (Mayo Clinic – Rochester, USA). NG,NG-dimethyl-L-arginine-3,3,4,4,5,5-2H6 was synthesized in our laboratory as described elsewhere (Schwedhelm E, 2007). Ammonia

solution, HPLC grade methanol and acetonitrile were purchased from Merck (Darmstadt, Germany).

Mass spectrometric analyses were performed using an Acquity UPLC Waters (Manchester, England) coupled with a Micromass Quattro Ultima triple quadrupole mass spectrometer (Waters Co., Milford, USA) equipped with an electrospray ion source operating in positive mode. Data were acquired with MassLynx 4.1 software and processed for calibration and quantification of the analytes with QuanLynx supplied by Waters Technical Services (Etten-Leur, NL). Analytical column used for separation was UPLC BEH C18 (1.7μm, 2.1×50mm) from Waters Co. The chromatographic run was performed at 600μLmin−1 with a gradient elution of a mobile phase which consisted of Solution A (water with 0.1% formic acid, v v−1) and Solution B (methanol with 0.1% formic acid, v v−1). The percentage of organic modifier was changed linearly as follows: 0 min, 2%; 0.21 min, 10%; 1.28 min, 50%; 1.81 min, 2%. Total analysis run time was 1.9 min. The injection volume was 6μL. Flow to the MS source was reduced by splitting 1:10 with a split tee positioned after column, in order to optimize ionization.

Internal standard solution was prepared by diluting 3μM of 13C,2H4-arginine, 2H2-citrulline and 2H6-ADMA in methanol and 150μL was added to each sample. Calibration has been achieved by applying the stable isotope dilution method. To assess linearity calibration curves in water, plasma and serum, were obtained adding increasing concentrations of ADMA, SDMA, NMMA and homo-arginine (0.05, 0.1, 0.5, 1, 2, 4μM) and of L-arginine and L-citrulline (0.5, 1, 25, 50, 100, 250μM). The endogenous concentrations of the analytes in all matrices were calculated using the intercept value to y-axis of calibration curves, using peak area ratios of the analytes to internal standard.

150μL of internal standard in methanol were added to 10μL of serum and centrifuged at 13,000 rpm for 10 min to remove the precipitated proteins. The supernatant was collected and dried under a nitrogen flow at 60°C.

Derivatisation step was performed dissolving the dried extract in 100μL of a freshly prepared butanol solution containing 5% (vv−1) acetyl chloride and kept at 60℃ for 20 min. The solvent was removed by evaporation under nitrogen flow at 60℃. The derivatised samples were dissolved in 50μL of water–methanol (90:10, vv−1) containing 0.1% (vv−1) formic acid and injected into the UPLC analytical column for chromatography. Multiple reaction monitoring (MRM) measurements were performer using optimal cone and collision energy values derived from preliminary fragmentation studies with a continuous infusion of a 50μM solution of each analyte.

Data analysis and statistics

Data are given as means ± SE. Scatter-plot graphics were made for spectrometry data distribution. Differences were analyzed using ANOVA test and the Neuman-Keuls multiple comparison test, or unpaired T-test were assessed, when indicated. A p value <0.05 was considered statistically significant (GraphPad Prism 5.04 Software, San Diego, USA).

Results

The technique of intra amniotic injection of LPS for chorioamnionitis induction is presented in the figure below.

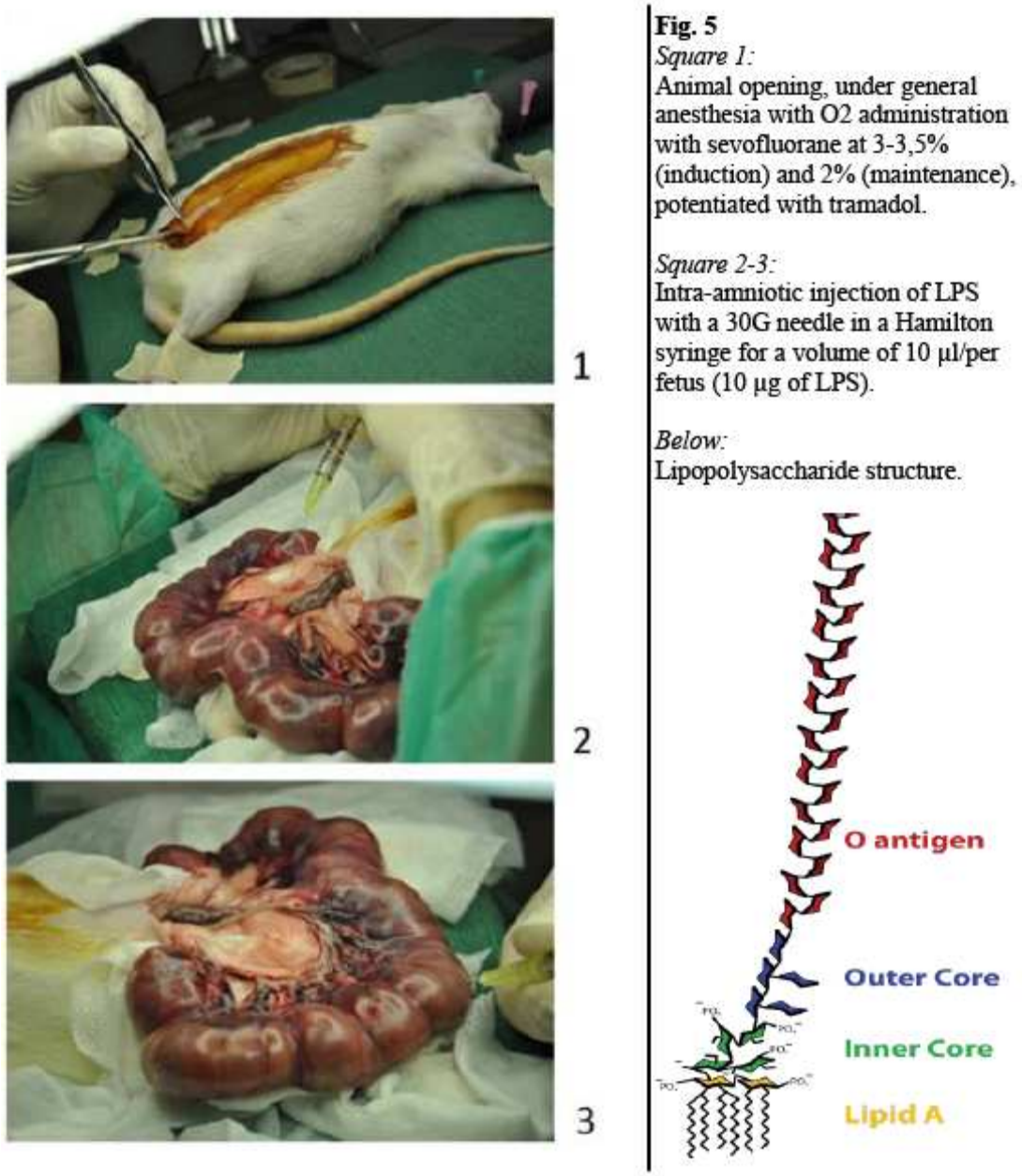

Fig. 5
Square 1:
Animal opening, under general anesthesia with O2 administration with sevofluorane at 3-3,5% (induction) and 2% (maintenance), potentiated with tramadol.

Square 2-3:
Intra-amniotic injection of LPS with a 30G needle in a Hamilton syringe for a volume of 10 µl/per fetus (10 µg of LPS).

Below:
Lipopolysaccharide structure.

Birth mortality and body weight

Those groups where LPS was used to induce chorioamnionitis presented at birth (within 24h from delivery) a mortality rate of 40%. Such a rate did

not change when we decided to use foster mothers, immediately after birth. Birth mortality was around 20% in the case when saline solution was administered (as control). No mortality was found in any group starting from postnatal day 2.

Body weight of the animals grew progressively from P1 through P14 (Fig. 6). In particular, at P10, body weight was increased in LPS+CITR group *vs.* all the other groups (**p<0.0001). Body weight was also increased in CITR+hyperoxia *vs*. Hyperoxia group (*p<0.005). In the same manner, at P14 body weight in LPS+CITR group was increased *vs.* all other groups (§ p<0.005), while no differences between LPS and Hyperoxia groups were observed.

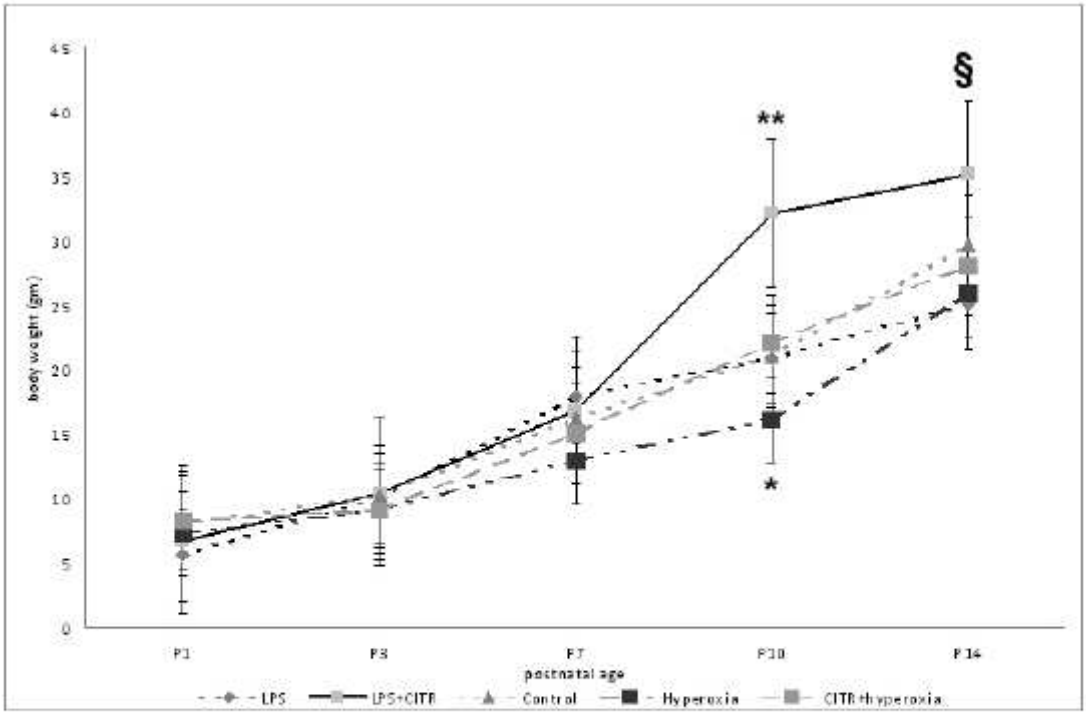

Fig. 6 Effects of intra-amniotic LPS and moderate postnatal hyperoxia on body weight of infant rats. As shown, at P10, body weight was increased in LPS+CITR group *vs.* all other groups (** $p < 0.0001$); body weight was also increased in CITR+hyperoxia *vs.* hyperoxia group (* $p < 0.005$). At P14 body weight in LPS+CITR group was increased *vs.* all other groups (§ $p<0.005$).

Lung histopathologic analysis

Figure 7, Figure 8 and Table 1 summarize the lung histopathology analysis. In particular, in the Figure 7 lungs under postnatal moderate

hyperoxia present a pattern typically emphysematous, with large air spaces and disruption of capillary endothelial barrier. This profile was similar to the LPS antenatal exposure group, when compared to the Control group. Exposure to FiO2=0.6 up to P14 was associated with an arrested alveolarization, inducing a change in lung morphology with patchy areas of parenchymal thickening interspersed with areas of enlarged air spaces. The lung sections of the CITR+hyperoxia and LPS+CITR rats contained smaller and more numerous air spaces, and were more similar to the lungs of the Control group. There was no evidence of inflammatory cells, but the septa were thicker in the Hyperoxia group than in the Control and CITR+hyperoxia groups.

In Figure 8, the time course examination from P7 to P14 of the lungs demonstrates an important arrest of the lung development. Particularly, at P7 and P10 lung architecture is compromised with evident hemorrhagic areas. Moreover, the alveolar walls were thickened and the septa seem edematous in the P7 and P10 microphotographs. Finally, the lung sections of the LPS+CITR or CITR+hyperoxia treated rats, contained smaller and more numerous air spaces, and were more similar to the lungs of the Control group and there was no evidence of inflammatory cells.

In Table 1 we show morphometric analyses counts. Specifically, the mean alveolar size (mm^2) at P14 was higher in Hyperoxia group (*) (1.56±0.16) *vs.* Control group (0.98±0.09) or LPS+CITR (0.82±0.1); in a *post hoc* comparison unchanged with respect to CITR+hyperoxia (1.39±0.17) or LPS (0.74±0.04) or CITR (1.03±0.05) – the latter histology was not shown – p=0.0001.

The mean linear intercept (μm) was lower in the LPS+CITR group (*) (35.92±1.81) than in the LPS (144.3±3.31) or Hyperoxia (77.91±6.25) or Control (66.19±7.50) groups, while CITR (§) (44.64±2.66) differed from that of Hyperoxia or LPS groups, and Hyperoxia (**) showed higher values when compared to Control or LPS ones, CITR+hyperoxia was 50.5±1.38; p=0.0001.

The secondary crests (n/hpf) were higher in the Control (74.7±3.12) and CITR+hyperoxia (66.17±0.6) and LPS+CITR (64.75±6.29) groups than in the Hyperoxia (*) (36.57±4.21) or LPS (*) (29.36±2.58) or CITR (*) (44.71±4.34) groups, p=0.0001.

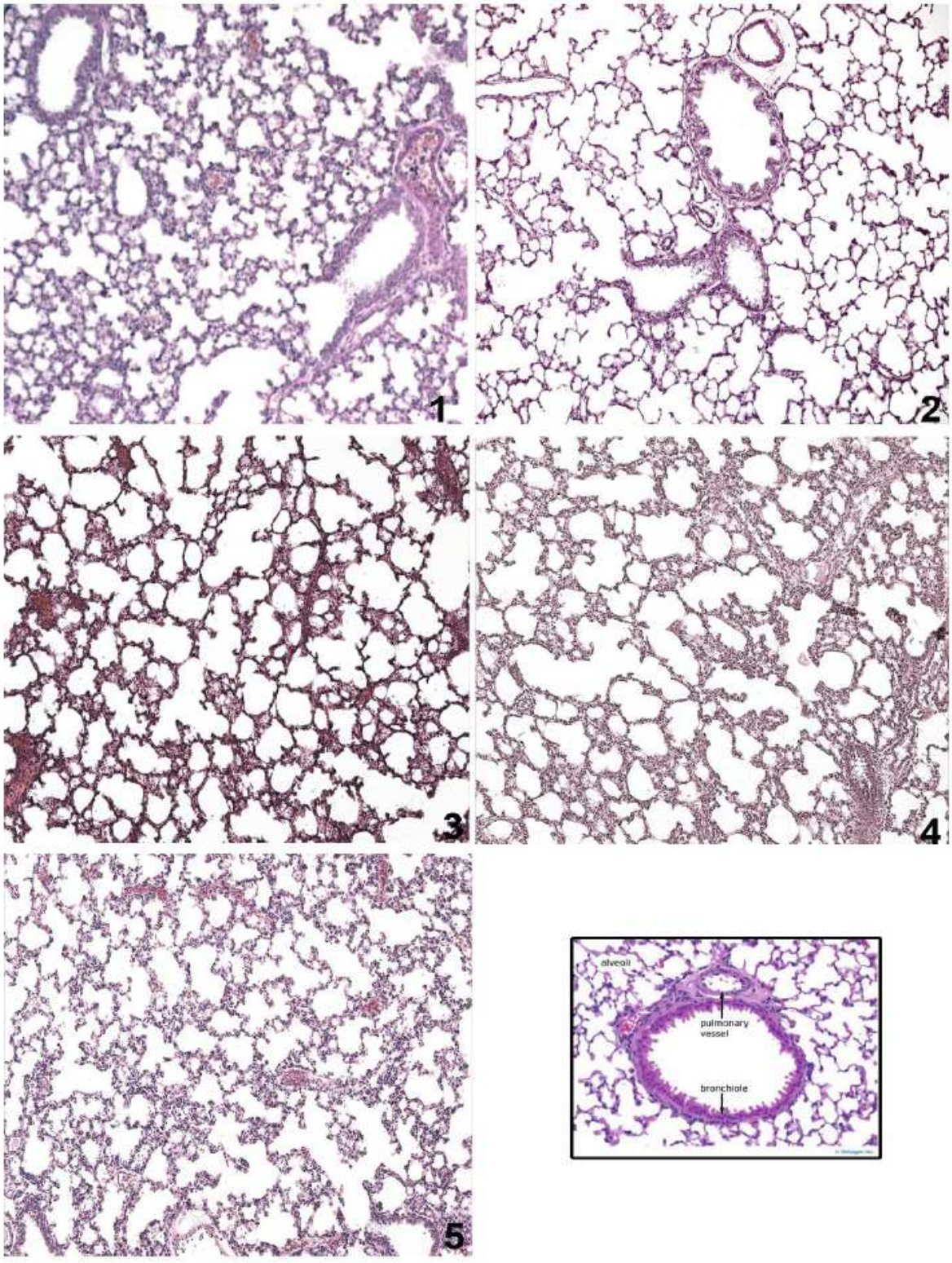

Fig. 7 Representation of H&E-stained lung sections at P14. *Square 1*: Morphometry from LPS-administered group; *Square 2*: Control group; *Square 3*: LPS+CITR group; *Square 4*: Hyperoxia group; *Square 5*: CITR+Hyperoxia group. Particular, is a representative section showing the relation between bronchiole, pulmonary vessels and alveoli (*from* Deltagen Inc.) Magnification 10X.

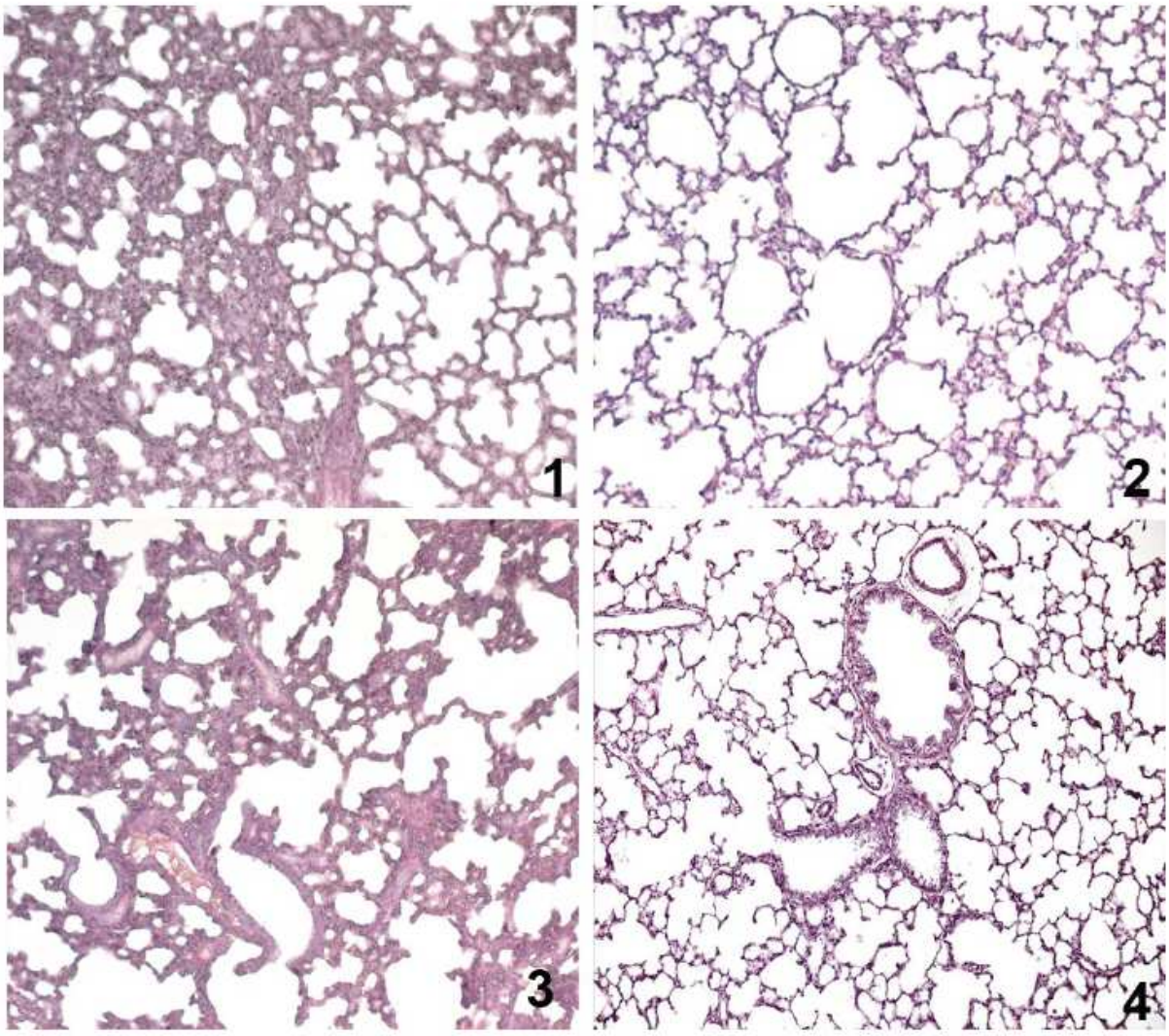

Fig. 8 Representation of H&E-stained lung sections showing the morphology of Group 2 (LPS-administered animals) at various time-points. *Square 1:* LPS group at P7; *Square 2:* LPS group at P14; *Square 3:* LPS group at P10; *Square 4:* Control group at P14. Magnification 10X.

Morphometric Analysis

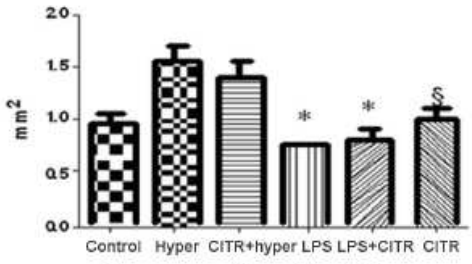

Average Alveolar Size

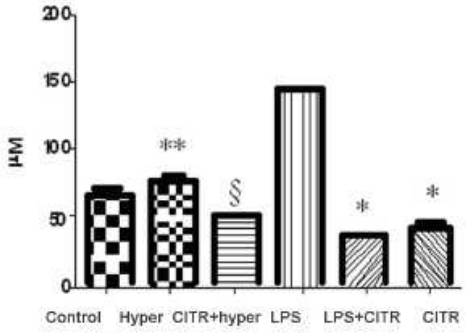

Mean Linear Intercept

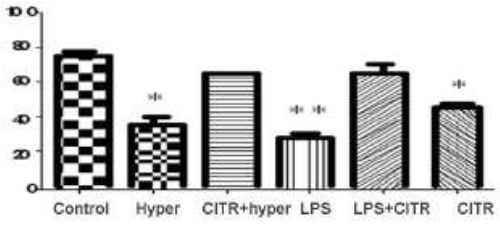

Secondary crests count

Tab. 1 Morphometric analysis on lung sections at P14. Statistics: *Average Alveolar Size:* * LPS or LPS+CITR or Control *vs.* Hyperoxia and CITR+hyperoxia, § CITR *vs.* Hyperoxia, $p<0.0001$.
Mean Linear Intercept: * LPS+CITR or CITR *vs.* Hyperoxia or *vs.* Control or *vs.* LPS, § CITR+hyperoxia *vs.* Hyperoxia or LPS, ** Hyperoxia or Control *vs.* LPS, $p<0.0001$.
Secondary crests count: * LPS (** LPS *vs.* CITR) or Hyperoxia *vs.* Control or CITR+hyperoxia or LPS+CITR, $p<0.0001$.

Effects of L-citrulline on alveolar endothelial barrier

VEGF (%) gene expression evaluated by real-time quantitative PCR (Fig. 9, Section 1). It was lower in the Hyperoxia group, than in the CITR+hyperoxia or Control groups, p<0.05. The values were as follows: Control=100±15.74%/GAPDH; Hyperoxia=54.81±3.28%/GAPDH;

CITR+hyperoxia=75.71±5.28%/GAPDH. A parallel result was obtained with Western blot performed on protein extracts. As shown in the graph with densitometric values (mean ± SE) normalized to GAPDH (Fig. 9, Section 2), protein expression was lower in the Hyperoxia group (0.07±0.02), than in the CITR+hyperoxia (0.13±0.02) and Control (0.15±0.01) groups, $p<0.05$.

To further analyze the relationship between VEGF expression and endothelial cells in the angiogenic process, we performed a specific vWF stain that identifies the endothelial vessel structures. As shown, lung sections from Control and CITR+hyperoxia animals showed a similar vWF expression, whereas staining was weaker in the Hyperoxia group (not shown). In the CITR+hyperoxia sections there was also evidence of a better organization of the vessel network than in the other animals exposed to hyperoxia, where it appeared more severely deranged. The graph in Figure 9, Section 3 shows the lung vessel density. In the CITR+hyperoxia group, the number of vessels returned to <100 μm/hpf (23±5), as seen in the Control group (17±7), as opposed to 13.7±3.5 in the Hyperoxia group ($p<0.05$).

The protein expression of eNOS was evaluated and normalized to GAPDH using Western blot analysis. As shown in Figure 9, Section 1 and 2, the amount of eNOS protein (mean ± SE) normalized in the lung tissue from the L-citrulline treated animals (1.08±0.22) was higher than in the tissues from the Hyperoxia group (0.77±0.11), $p<0.05$, in which there was an increase by comparison with the Control group (0.33±0.09), $p<0.05$.

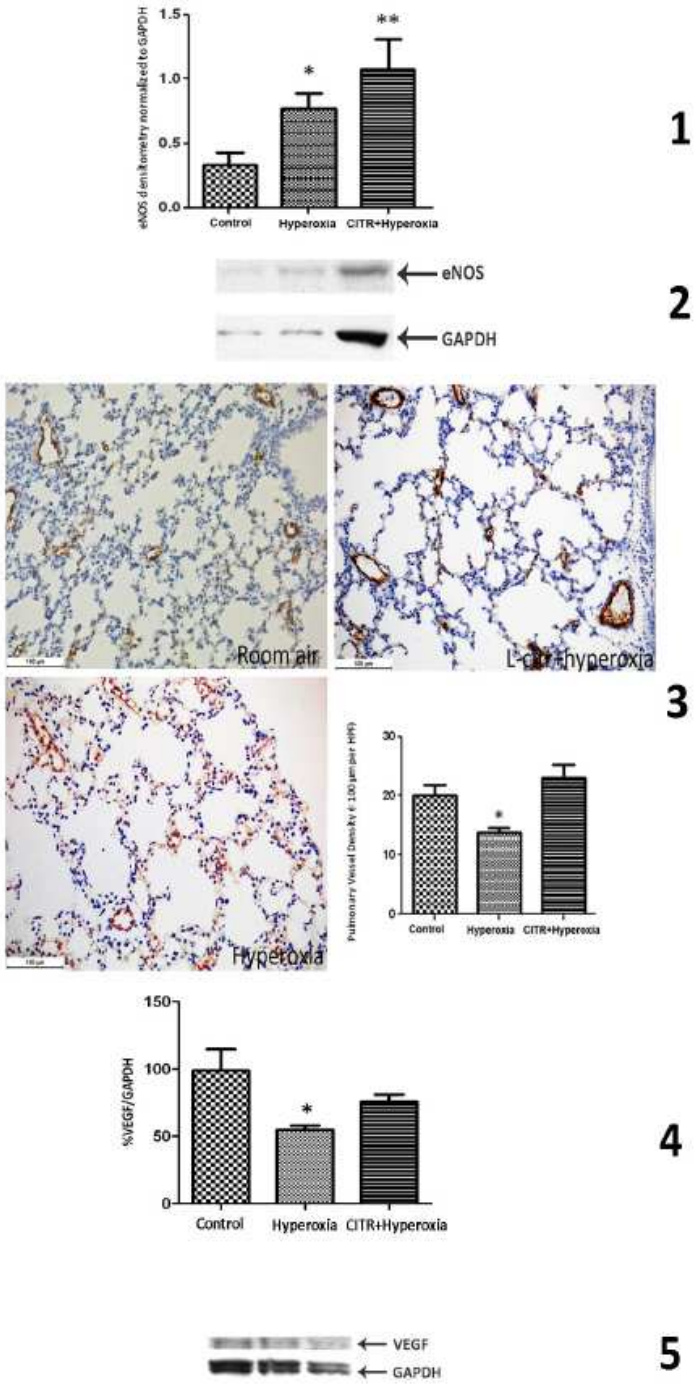

Fig 9 Effects of CITR and LPS on the alveolar endothelial barrier

Section 1 and 2:
Western blot analysis of lung tissue * indicates that eNOS protein expression was higher in the hyperoxia group than in the Control group, $p<0.05$;
** indicates that eNOS protein expression was higher in the CITR+hyperoxia group than in the other groups, $p<0.05$.

Section 3:
Immunohistochemistry of vWF expression in lung tissue and pulmonary vessel density shows the effect of L-citrulline treatment on angiogenesis. Magnification 20X. The number of vWF-positive vessels (<100 µm in size) was counted per hpf. The CITR+hyperoxia group had the same number of vessels as in the Control group.
* indicates that the hyperoxia group had fewer vWF-positive vessels than the CITR+hyperoxia and Control groups, $p<0.05$.

Sections 4 and 5:
Real-time PCR analysis of pulmonary VEGF gene expression and Western blot analysis on VEGF protein expression.
* indicates that VEGF expression was lower in the hyperoxia group than in the Control and CITR+hyperoxia groups, $p<0.05$.

Mass spectrometric analyses

Here we have summarized the available variables that link ADMA with chorioamnionitis disease and give the L-arginine, L-citrulline, and

asymmetric methylarginines, (ADMA, NMMA and SDMA), plus homo-arginine, in a time related pattern as well as under LPS and/or L-citrulline treatment. It is noteworthy that the treated groups do not show differences in the time course and treatment groups.

In Group 1 (LPS+CITR), at P14, ADMA, SDMA and L-citrulline serum levels were statistically different *versus* the other time-points; whereas L-arginine at P10 and P14 was statistically different *versus* P3.

In Group 2 (LPS alone), ADMA serum levels at P14 were statistically different *versus* all the other time-points. SDMA levels at P14 were as well statistically different *versus* P10 and P7. On the other hand, L-citrulline levels were statistically different at P7 *versus* the other time-points; finally no substantial difference was observed regarding the L-arginine levels.

In Group 7 (Control), ADMA levels were not statistically different in the various time-points; while P3 levels of SDMA were statistically different *versus* P10 and P14. The same, L-arginine serum levels at P14 were statistically different *versus* P3 and P7. No significance was noted for the L-citrulline levels.

In Group 8 (Control+CITR), ADMA levels were not statistically different at various time-points; while P14 levels were statistically different *versus* P3 and P10; the same, L-citrulline levels were statistically different *versus* the other time-point serum levels.

A confront in a single time-point (P7) was made between animals receiving LPS+hyperoxia, with or without L-citrulline treatment (Group 5 and 6 – *see* Experimental Design). No statistically difference was noticed in spectrometric assessment between these groups at P7.

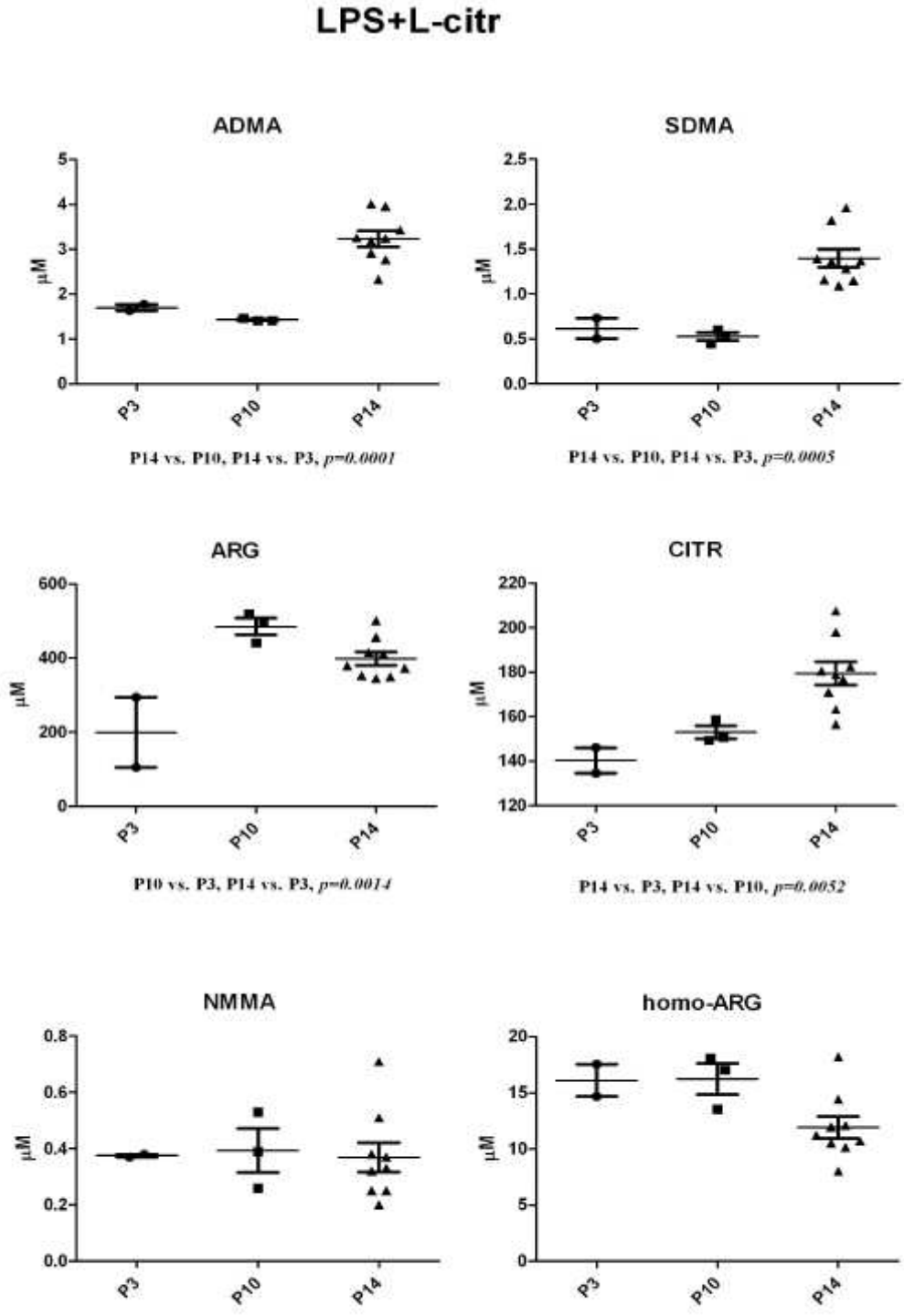

Fig. 10 Serum Asymmetric dimethylarginine (ADMA), Symmetric dimethylarginine (SDMA), L-Arginine (ARG), L-citrulline (CITR), N^G – monomethyl-L-arginine (NMMA), Homoarginine (homo-ARG) assessment in rats of Group 1 (*see* experimental design)

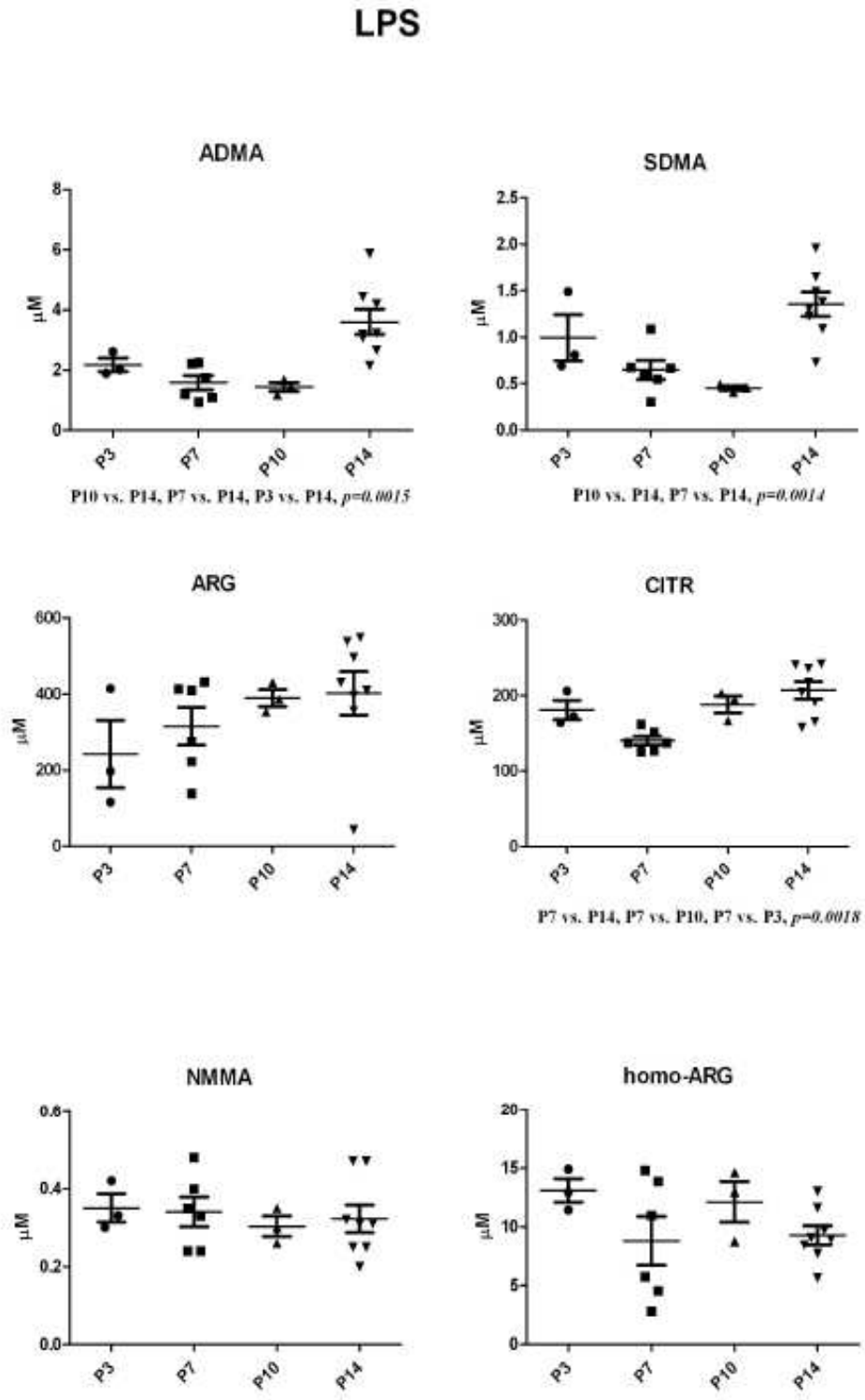

Fig. 11 Serum ADMA, SDMA, ARG, CITR, NMMA, homo-ARG assessment in rats of Group 2 (*see* experimental design)

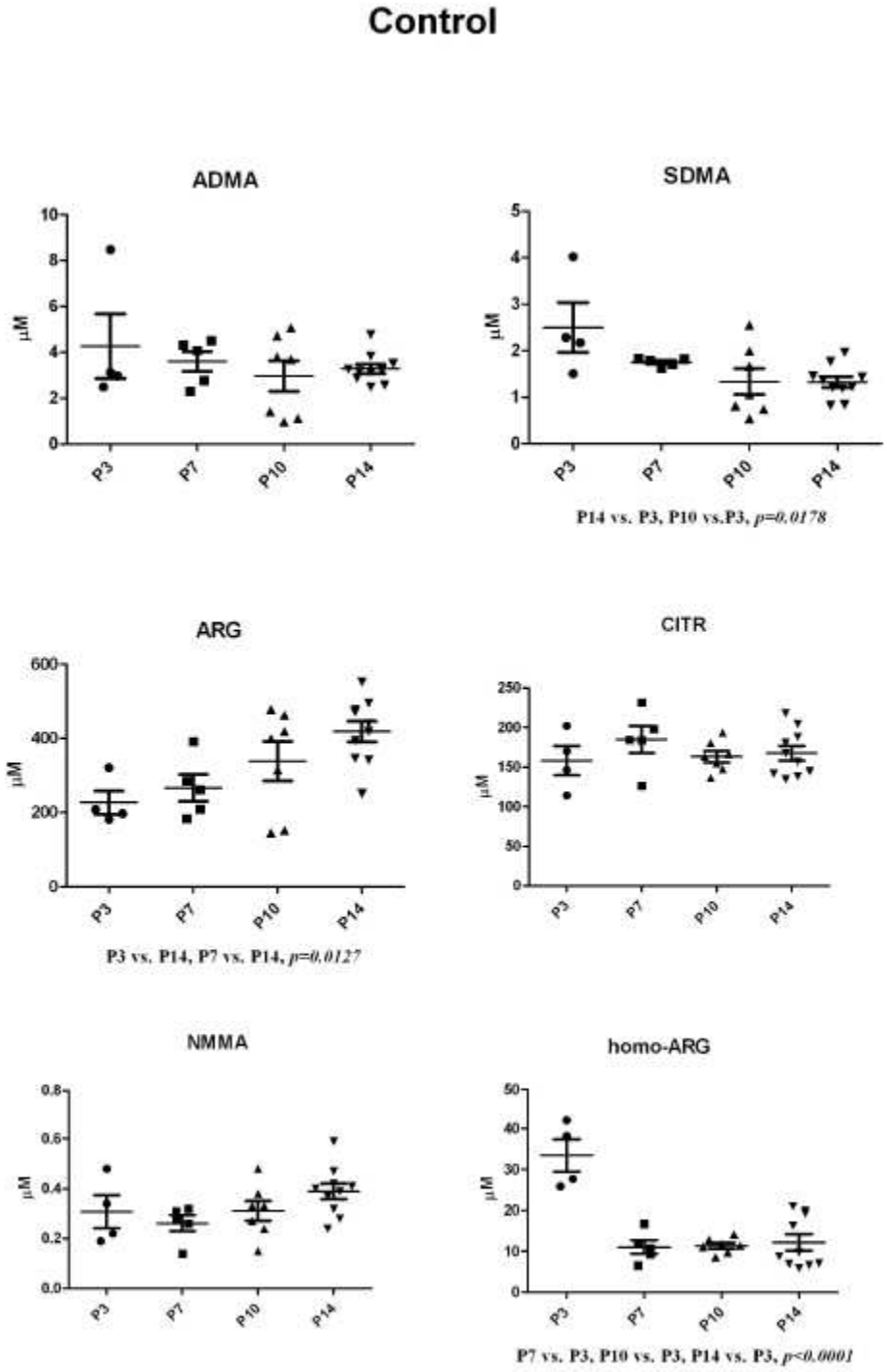

Fig. 12 Serum ADMA, SDMA, ARG, CITR, NMMA, homo-ARG assessment in rats of Group 7 (*see* experimental design)

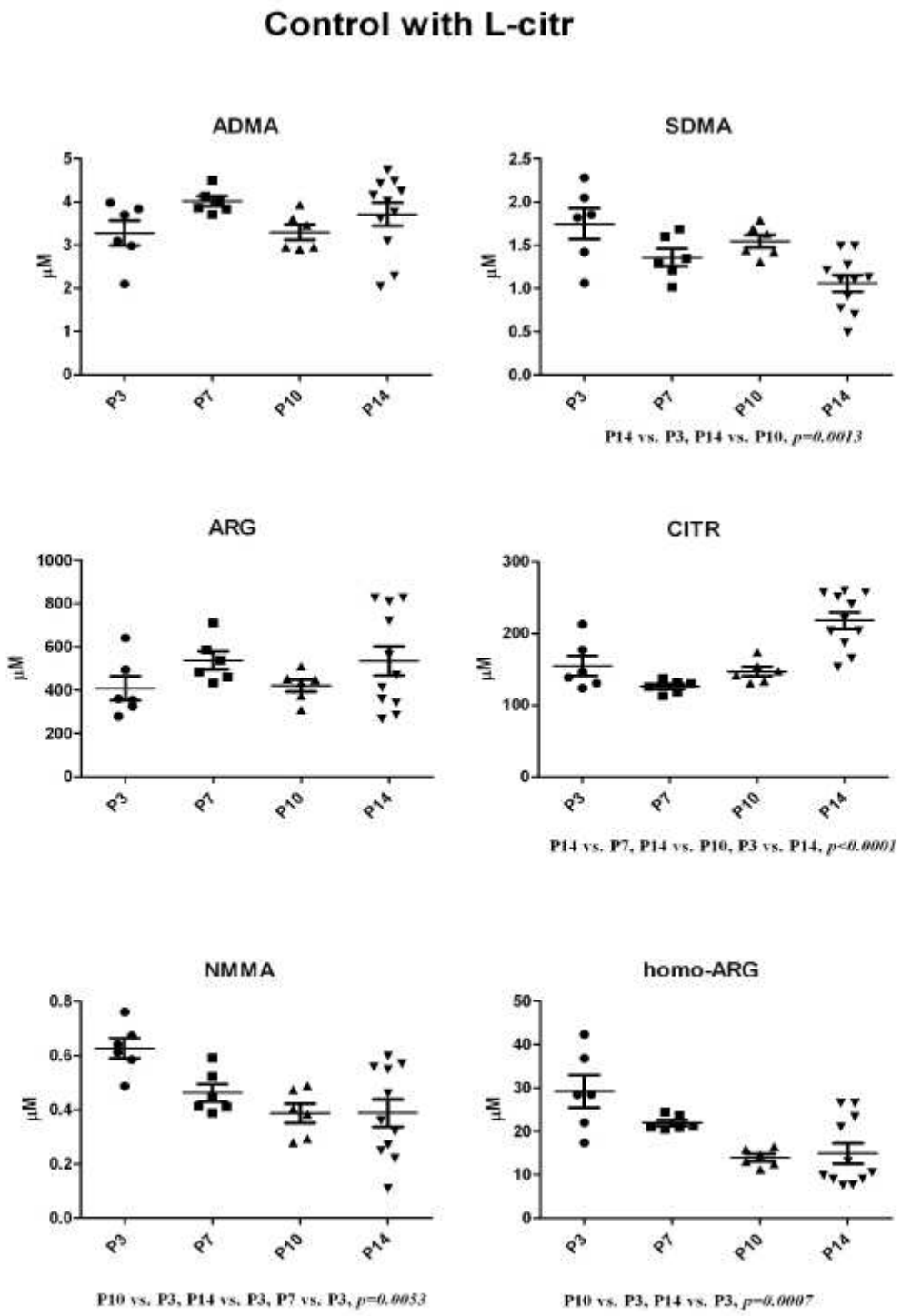

Fig. 13 Serum ADMA, SDMA, ARG, CITR, NMMA, homo-ARG assessment in rats of Group 8 (*see* experimental design)

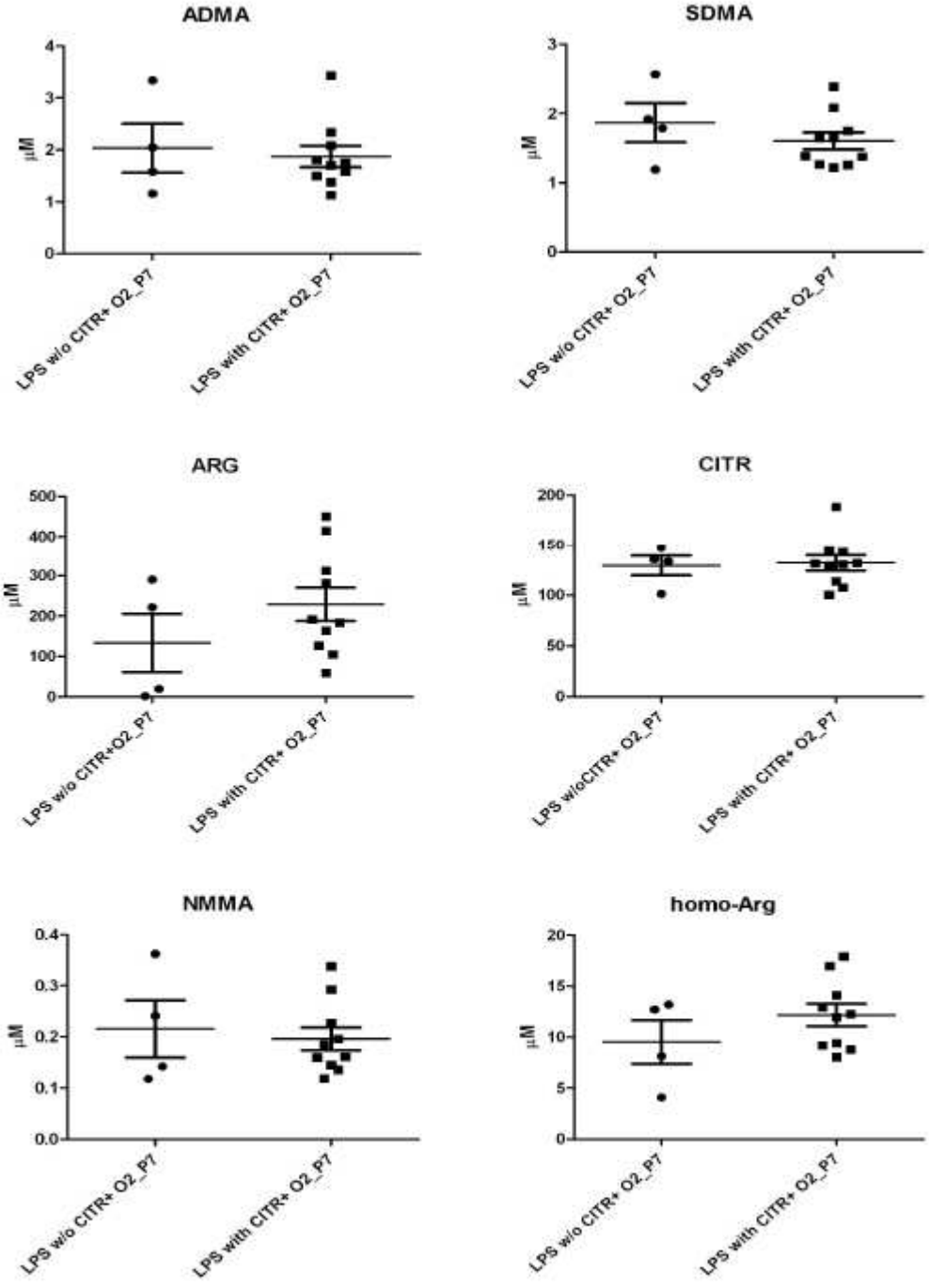

Fig. 14 Comparison at P7 between serum values of ADMA, SDMA, ARG, CITR, NMMA and homo-ARG (Group 5 and 6, *see* experimental design).

Discussion

We administered L-citrulline for two weeks in newborn rats exposed to moderate hyperoxia and in a model of pulmonary inflammation and sufferance of experimental chorioamnionitis, exposing fetal rats to a single dose of intra-amniotic endotoxin LPS.

Previous studies shown strong association of chorioamnionitis with BPD, but recently other papers fail to demonstrate an increase in the incidence of BPD in premature infants who were exposed to chorioamnionitis (Andrews *et al*, 2006; Dempsey *et al*, 2005; Kaukola *et al*, 2009; Kent & Dahlstrom, 2004). Clinical observations have generated the concept that antenatal exposure to inflammation may have positive and/or negative effects on preterm lung function and development (Been & Zimmermann, 2009; Kumar *et al*, 2008). Thus, we chose a consolidated animal model (Kim *et al*, 2010; Flam *et al*, 2007) to study how fetal exposure to inflammation affects the lung. Rat lungs differ from human lungs because they do not present alveoli at birth – it is thought that they develop rapidly between days 4 and 14 postnatally, although older data indicate that this continues to occur until 4 weeks of age (Holmes & Thurlbeck, 1979). Blanco and Frank (Blanco & Frank, 1994), using modern stereological methods, showed that the number of alveoli doubled between 14 and 28 days of age and continued to increase more slowly to 60 days of age. Typical alveoli are readily apparent at 36 weeks of gestation in all human fetuses (Langston *et al*, 1984) and other observers have recognized alveoli even earlier (Hislop *et al*, 1986). We therefore thought to investigate four time-points coinciding with passages to different phases of lung maturation in rats and in humans from saccular (P7) to canalicular (P10) and alveolar stage (P14). Due to the invasiveness of the model we had several difficulties to have enough newborn rats to cover homogenously all the trials of the experimental design. A mortality of pups at birth around 40%

was noticed (within 24h from delivery) only in those groups where LPS was used to induce chorioamnionitis. As hypothesized, this mortality did not change when we decided to use foster mothers, immediately after birth and, interestingly, birth mortality was around 20% when saline solution was administered (as control). Anyway no mortality was found in any group beginning postnatal day 2. All animals gained weight along 14 days but significant differences at P10 and at P14 in groups of animals receiving L-citrulline support the positive effect of treatment on the wellness of rats.

Since LPS and hyperoxia deeply alter the normal morphology of the lungs we performed H&E histopathological evaluations with contextual assessment of morphometric parameters MLI, average alveolar size and number of secondary crests that are well described in literature (Balasubramaniam *et al*, 2007). The marked reduction in alveolarization and vascular growth led to altered lung structure. It is well known that alveolar barrier disruption leads to pulmonary hypertension and right ventricular hypertrophy that we didn't evaluate due to complexity to collect enough tissues and specimens for all evaluations. Anyway, mortality rate and derangement in normal pulmonary vascular growth and structure in our model suggest that intrauterine inflammation may be sufficient to induce prolonged impairment of vascular growth and structure characteristic of BPD and may contribute to the pathogenesis of neonatal pulmonary hypertension reported in literature.

Hyperoxia and oxidative stress have been shown to be major risk factors for the development of BPD in various studies. Previously, it has been reported that severe neonatal hyperoxia worsens the impairment of neonatal lung growth after antenatal inflammation due to intra-amniotic infection (Choi *et al*, 2009; Normann *et al*, 2009; Velten *et al*, 2010). Tang *et al*, in their work of 2010, reported instead that moderate hyperoxia accelerates lung growth and attenuates pulmonary hypertension after intra-amniotic endotoxin exposure. This is surprisingly in contrast with our data presented here, which give evidence that hyperoxia and LPS exposure

and/or a combination of both these stimuli, produce significant changes in the average alveolar size of animals exposed to hyperoxia and LPS. During the first 2-3 days of postnatal life, alveolar primary saccule enlarges by the development of secondary crests and is then subdivided into alveoli. Our findings suggest that LPS and hyperoxia may cause an important arrest of maturation of the alveolar barrier, since the secondary crests count was significantly lower in LPS and hyperoxia group. Finally, significant changes of mean linear intercept in the lung of LPS and hyperoxia exposed animals suggested the extent of large surfaces of emphysema.

Growth in lung circulation and alveolarization are closely coordinated events, occurring throughout lung morphogenesis (Jakkula *et al*, 2000) and NO has proved to be a crucial regulator of lung morphogenesis and homeostasis in fetal life (McCurnin *et al*, 2005). NO improves gas exchange, reduces lung inflammation and oxidant stress, and enhances angiogenesis and growth in the immature lung. It also prolongs survival in an animal model of BPD (ter Horst *et al*, 2007). Oral supplementation with L-arginine has been shown to enhance NO-mediated vasodilatation in several (Bode-Böger *et al*, 2003; Piatti *et al*, 2001), but not in all clinical studies (Walker *et al*, 2001). Unfortunately, L-arginine is subject to extensive pre-systemic and systemic elimination, i.e. by bacteria in the gut, and arginases in the gut and liver, respectively (Curis *et al*, 2005), whereas the non-essential amino acid L-citrulline is not subject to pre-systemic elimination; it is converted into L-argininosuccinate by argininosuccinate synthase and, subsequently, into L-arginine by argininosuccinate lyase (Schwedhelm *et al*, 2008). It may therefore serve as an L-arginine precursor (Solomonson *et al*, 2003), and many NO producing cells (vascular endothelial cells and macrophages) use L-citrulline as a substrate to form L-arginine. Oral L-citrulline supplementation raises plasma L-arginine concentrations and increases NO-dependent signaling in a dose-dependent manner. It has been shown that providing L-arginine

to endothelial cells increases NO production, but only slightly by comparison with the more dramatic increase induced by L-citrulline supplementation (Greeenle *et al*, 2007). We hypothesized that administering L-citrulline, and thereby raising serum levels of L-arginine, might attenuate hyperoxia and/or LPS lung damage.

In particular, at P14 we found encouraging changes in the lung morphology of the rats under hyperoxia or LPS given L-citrulline, which seemed to have a protective effect, by improving alveolarization, as demonstrated by the smaller mean linear intercept and the larger number of secondary crests. Moreover, a decreased mean alveolar size would also be indicative of a smaller emphysematous surface, as compared to the other investigated groups (LPS or Hyperoxia). This preliminary finding prompted us to study specific markers of lung development, to better characterize the effects of L-citrulline. In particular, VEGF plays a crucial role in the proper metabolism of the endothelial and alveolar barrier; it is a potent pro-angiogenic and endothelial survival factor (Balasubramaniam et al, 2007; Balasubramaniam & Ingram, 2009). A finding worthy to emphasize in our results was the return to a normal level of VEGF expression in the L-citrulline treated lung, which reached the same level as in the Control group, while it was lower in the untreated groups exposed to hyperoxia. This result was confirmed by the higher prevalence of VEGF-positive cells found in the lungs of the treated animals than in those untreated. It has been reported that NO is a powerful downstream VEGF controller (Jobe & Bancalari, 2001), but the exact relationship between NO and VEGF is still not clear, since it appears that NO might also take effect upstream from the VEGF (Duda *et al*, 2004). Based on our findings, we speculate that in our model the endogenous NO (presumably obtained from L-citrulline administration as well as from its metabolism to L-arginine) looks more like an upstream than a downstream mediator. Further studies are needed to understand the factors regulating NO/VEGF signaling and L-citrulline administration. Alveolarization is known to require coordination between

several factors, particularly an optimal interaction between extracellular matrix remodeling and epithelial morphogenesis and capillary growth (Ziche *et al*, 1997).

Evidences suggest that lung structure and function are partly maintained by a balance between the competing arginine-metabolizing enzymes arginase and nitric oxide synthase. ADMA is an endogenous inhibitor of NO synthase. ADMA is formed as a metabolic by-product of continuous protein turnover in all cells of the body. For example, significant increased lung ADMA concentrations were associated with acute lung-injury collagen deposition (Sousse *et al*, 2011) and with idiopathic pulmonary arterial hypertension (IPAH) (Kielstein & Cooke, 2005). Therefore, we have evaluated the available variables that link ADMA with chorioamnionitis disease and give the L-arginine, L-citrulline, and asymmetric methylarginines (ADMA, NMMA and SDMA), plus homo-arginine, in a time related pattern as well as under LPS and/or L-citrulline treatment. We proved that ADMA, maybe by inhibiting NO sinthases isoforms, could lead to the rise in L-arginine in a specular time related bioavailability. It is noteworthy that the treated groups do not show differences in the time course, whereas at P14 of the LPS+CITR group, ADMA, SDMA and L-citrulline serum levels were statistically different *versus* the other time-points. Furthermore, ADMA serum levels at P14 in the LPS group were statistically different *versus* all the other time-points.

The confront made at P7 between animals receiving LPS+hyperoxia, with or without L-citrulline treatment, displayed no statistical differences and this remains unexplainable.

It is important to note that the relative concentrations of ADMA and NMMA may differ between tissues and organ systems and hence the contribution of endogenously produced NMMA to NO bioavailability may be of more importance in certain tissues. It is worthy of note that the treated groups do not show differences in the time course. Our results also suggest that chorioamnionitis disease (untreated or under L-citrulline administration) on

the first 10 day period does not change the NMMA profile. SDMA, a stereoisomer of ADMA, does not directly inhibit NOS. SDMA agrees with the ADMA trend in the time related figure, as well as in the treatment related groups. Homo-arginine is a naturally occurring, basic, nonessential amino acid that is believed to be derived from lysine (Ryan & Wells, 1964). Homo-arginine has been detected in small amounts in all studied body fluids and organs (Meinitzer *et al*, 2007), but its function is not yet clearly resolved. Several functional studies have demonstrated that homo-arginine, in addition to L-arginine, can act as a substrate for NO production by NOS (Hrábak *et al*, 1994). Thus, homo-arginine may play a role in the regulation of NO release like a vasodilator (Bhardwaj & Moore, 1989). Our results show that homo-arginine increased in the P3 controls, but not in the LPS group or LPS+CITR group. It seems that this treatment counteracts the physiological rise in this amino acid level, highlighting its role in endothelial function across the pregnancy and thereby in the perinatal period. We have developed a rodent model of systemic maternal inflammation followed by neonatal oxidant stress. Our studies support the hypothesis that the combined effects of neonatal hyperoxia exposure and systemic maternal inflammation are responsible for a phenotype that shares many histological and pathophysiological characteristics of BPD, which include acute and prolonged alterations in lung structure and function. These findings imply that the combination of perinatal and postnatal insults may result in a worsen neonatal outcome than any single event taken alone. Furthermore, neonatal hyperoxia, in addition to systemic maternal inflammation, induces a fibrotic response and a BPD-like phenotype that closely mimics human disease.

Conclusions

In conclusion, our main findings were that: (i) administering L-citrulline proved effective in improving alveolar growth after oxygen-induced and antenatal endotoxin exposure lung damage; this might conceivably relate to the pathway of conversion into L-arginine. Mean serum L-arginine concentrations were higher in our L-citrulline treated group, which also revealed a better alveolar and vascular growth; (ii) VEGF gene and protein were over expressed in the group treated with L-citrulline. We speculate that the rise in VEGF/eNOS improved the upstream and downstream signaling events leading to the induction of neo-vascularization by NO in the L-citrulline treated group.

Bearing in mind that the main effect of L-citrulline is an increase in L-arginine levels, as a promoter and a substrate of eNOS, there may have been further protective effects on the alveolar vascular network and, consequently, on matrix maturation in our model, and this may be promising with a view to BPD prevention strategies.

References

Achan V, Broadhead M, Malaki M, Whitley G, Leiper J, MacAllister R, Vallance P. Asymmetric dimethylarginine causes hypertension and cardiac dysfunction in humans and is actively metabolized by dimethylarginine dimethylaminohydrolase. Arterioscler Thromb Vasc Biol. 2003 Aug 1;23(8):1455-9.

Alfiero Bordigato M, Piva D, Di Gangi IM, Giordano G, Chiandetti L, Filippone M. Asymmetric dimethylarginine in ELBW newborns exposed to chorioamnionitis. Early Hum Dev. 2011 Feb;87(2):143-5.

Andrews WW, Goldenberg RL, Faye-Petersen O, Cliver S, Goepfert AR, Hauth JC. The Alabama Preterm Birth study: polymorphonuclear and mononuclear cell placental infiltrations, other markers of inflammation, and outcomes in 23- to 32-week preterm newborn infants. Am J Obstet Gynecol. 2006 Sep;195(3):803-8.

Balasubramaniam V, Ingram DA. Endothelial progenitors in the risk of developing bronchopulmonary dysplasia: can we include endothelial progenitor cells in BPD risk assessment? Am J Respir Crit Care Med. 2009;180:488-90

Balasubramaniam V, Mervis CF, Maxey AM, Markham NE, Abman SH. Hyperoxia reduces bone marrow, circulating, and lung endothelial progenitor cells in the developing lung: implications for the pathogenesis of bronchopulmonary dysplasia. Am J Physiol Lung Cell Mol Physiol. 2007;292:L1073-84

Baraldi E, Filippone M. Chronic lung disease after premature birth. N Engl J Med. 2007 Nov 8;357(19):1946-55.

Been JV, Rours IG, Kornelisse RF, Lima Passos V, Kramer BW, Schneider TA et al. Histologic chorioamnionitis, fetal involvement, and antenatal steroids: effects on neonatal outcome in preterm infants. Am J Obstet Gynecol 2009; 201(6): 587.e1–587.e8.

Bhardwaj R, Moore PK. The effect of arginine and nitric oxide on resi stance blood vessels of the perfused rat kidney. Br J Pharmacol. 1989 Jul;97(3):739-44.

Blanco LN, Frank L. Development of gas-exchanging surface area in rat lung. The effect of alveolar shape. Am J Respir Crit Care Med. 1994;149:759–66.

Been JV, Zimmermann LJ. Histological chorioamnionitis and respiratory outcome in preterm infants. Arch Dis Child Fetal Neonatal Ed 2009; 94: F218–25.

Bode-Böger SM, Muke J, Surdacki A, Brabant G, Böger RH, Frölich JC. Oral l-arginine improves endothelial function in healthy individuals older than 70 years. Vasc Med. 2003;8:77–81.

Cherukupalli K, Larson JE, Puterman M, Sekhon HS, Thurlbeck WM. Comparative biochemistry of gestational and postnatal lung growth and development in the rat and human. Pediatr Pulmonol. 1997 Jul;24(1):12-21.

Choi CW, Kim BI, Hong JS, Kim EK, Kim HS, and Choi JH. Bronchopulmonary dysplasia in a rat model induced by intra-amniotic inflammation and postnatal hyperoxia: morphometric aspects. Pediatr Res. 2009;65: 323-7.

Closs EI, Basha FZ, Habermeier A, Förstermann U. Interference of L-arginine analogues with L-arginine transport mediated by the y+ carrier hCAT-2B. Nitric Oxide. 1997 Feb;1(1):65-73.

Cooke JP. NO and angiogenesis. Atheroscler Suppl. 2003 Dec;4(4):53-60.

Curis E, Nicolis I, Moinard C, Osowska S, Zerrouk N, Bénazeth S, Cynober L. Almost all about citrulline in mammals. Amino Acids. 2005 Nov;29(3):177-205.

Dempsey E, Chen MF, Kokottis T, Vallerand D, Usher R. Outcome of neonates less than 30 weeks gestation with histologic chorioamnionitis. Am J Perinatol. 2005 Apr;22(3):155-9.

Di Gangi IM, Chiandetti L, Gucciardi A, Moret V, Naturale M, Giordano G. Simultaneous quantitative determination of N(G),N(G)-dimethyl-L-arginine or asymmetric dimethylarginine and related pathway's metabolites in biological fluids by ultrahigh-performance liquid chromatography/electrospray ionization-tandem mass spectrometry. Anal Chim Acta. 2010 Sep 16;677(2):140-8.

Donohue PK, Gilmore MM, Cristofalo E, Wilson RF, Weiner JZ, Lau BD, Robinson KA, Allen MC. Inhaled nitric oxide in preterm infants: a systematic review. Pediatrics. 2011;127:e414-22.

Duda DG, Fukumura D, Jain RK. Role of eNOS in neovascularization: NO for endothelial progenitor cells. Trends Mol Med. 2004;10:143-5.

Faye-Petersen OM. The placenta in preterm birth. J Clin Pathol 2008; 61: 1261–75.

Figueras-Aloy J, Salvia-Roiges MD, Rodriguez-Miguélez JM, Miracle-Echegoyen X, Botet-Mussons F, Marín-Soria JL, Carbonell-Estrany X. Impact of chorioamnionitis on exhaled nitric oxide and endotracheal aspirate levels of nitrites-nitrates and interleukin-8 in mechanically ventilated preterm neonates. Pediatr Pulmonol. 2011 Jun;46(6):595-603.

Flam BR, Eichler DC, Solomonson LP. Endothelial nitric oxide production is tightly coupled to the citrulline-NO cycle. Nitric Oxide. 2007 Nov-Dec;17(3-4):115-21.

Gantert M, Been JV, Gavilanes AW, Garnier Y, Zimmermann LJ, Kramer BW. Chorioamnionitis: a multiorgan disease of the fetus? J Perinatol. 2010 Oct;30 Suppl:S21-30.

Goldenberg RL, Andrews WW, Goepfert AR, Faye-Petersen O, Cliver SP, Carlo WA, Hauth JC. The Alabama Preterm Birth Study: umbilical cord blood Ureaplasma urealyticum and Mycoplasma hominis cultures in very preterm newborn infants. Am J Obstet Gynecol. 2008 Jan;198(1):43.e1-5.

Goldenberg RL, Hauth JC, Andrews WW. Intrauterine infection and preterm delivery. N Engl J Med. 2000 May 18;342(20):1500-7.

Gorenflo M, Zheng C, Werle E, Fiehn W, Ulmer HE. Plasma levels of asymmetrical dimethyl-L-arginine in patients with congenital heart disease and pulmonary hypertension. J Cardiovasc Pharmacol. 2001 Apr;37(4):489-92.

Greenlee KJ, Werb Z, Kheradmand F. Matrix metalloproteinases in lung: multiple, multifarious, and multifaceted. Physiol Rev. 2007;87:69-98.

Guidolin D, Albertin G, Spinazzi R, Sorato E, Mascarin A, Cavallo D, Antonello M, Ribatti D. Adrenomedullin stimulates angiogenic response in cultured human vascular endothelial cells: involvement of the vascular endothelial growth factor receptor 2. Peptides. 2008;29:2013-23.

Holmes C, Thurlbeck WM. Normal lung growth and response after pneumonectomy in rats at various ages. Am Rev Respir Dis. 1979;120:1125–36.

Hislop AA, Wigglesworth JS, Desai R. Alveolar development in the human fetus and infant. Early Hum Dev. 1986; 131-41.

Hrabák A, Bajor T, Temesi A. Comparison of substrate and inhibitor specificity of arginase and nitric oxide (NO) synthase for arginine analogues and related compounds in murine and rat macrophages. Biochem Biophys Res Commun. 1994 Jan 14;198(1):206-12.

Husain AN, Siddiqui NH, Stocker JT. Pathology of arrested acinar development in postsurfactant bronchopulmonary dysplasia. Hum Pathol. 1998;29:710–7.

Jakkula M, Le Cras TD, Gebb S, Hirth KP, Tuder RM, Voelkel NF, Abman SH. Inhibition of angiogenesis decreases alveolarization in the developing rat lung. Am J Physiol Lung Cell Mol Physiol. 2000 Sep;279(3):L600-7.

Jobe AH, Bancalari E. Bronchopulmonary dysplasia. Am J Respir Crit Care Med. 2001;163:1723–29.

Kakimoto Y, Akazawa S. Isolation and identification of N-G,N-G- and N-G,N'-G-dimethyl-arginine, N-epsilon-mono-, di-, and trimethyllysine, and glucosylgalactosyl- and galactosyl-delta-hydroxylysine from human urine. J Biol Chem. 1970 Nov 10;245(21):5751-8.

Katz JE, Dlakić M, Clarke S. Automated identification of putative methyltransferases from genomic open reading frames. Mol Cell Proteomics. 2003 Aug;2(8):525-40.

Kaukola T, Tuimala J, Herva R, Kingsmore S, Hallman M. Cord immunoproteins as predictors of respiratory outcome in preterm infants. Am J Obstet Gynecol. 2009 Jan;200(1):100.e1-8.

Kelly NM, Young L, Cross AS. Differential induction of tumor necrosis factor by bacteria expressing rough and smooth lipopolysaccharide phenotypes. Infect Immun. 1991;59: 4491–6.

Kent A, Dahlstrom JE. Chorioamnionitis/funisitis and the development of bronchopulmonary dysplasia. J Paediatr Child Health. 2004 Jul;40(7):356-9.

Kielstein JT, Cooke JP. Arginine metabolism, pulmonary hypertension, and sickle cell disease. JAMA. 2005;Nov 16;294(19):2433; author reply 2433-4.

Kim DH, Choi CW, Kim EK, Kim HS, Kim BI, Choi JH, Lee MJ, Yang EG. Association of increased pulmonary interleukin-6 with the priming effect of intra-amniotic lipopolysaccharide on hyperoxic lung injury in a rat model of bronchopulmonary dysplasia. Neonatology. 2010 Jun;98(1):23-32.

Kim YJ, Park HS, Lee HY, Ha EH, Suh SH, Oh SK, Yoo HS. Reduced L-arginine level and decreased placental eNOS activity in preeclampsia. Placenta. 2006 Apr-May;27(4-5):438-44.

Kumar R, Yu Y, Story RE, Pongracic JA, Gupta R, Pearson C et al. Prematurity, chorioamnionitis, and the development of recurrent wheezing: a prospective birth cohort study. J Allergy Clin Immunol 2008; 121: 878–84 e876.

Lahra MM, Beeby PJ, Jeffery HE. Maternal versus fetal inflammation and respiratory distress syndrome: a 10-year hospital cohort study. Arch Dis Child Fetal Neonatal Ed. 2009 Jan;94(1):F13-6.

Lahra MM, Beeby PJ, Jeffery HE. Intrauterine inflammation, neonatal sepsis, and chronic lung disease: a 13-year hospital cohort study. Pediatrics. 2009 May;123(5):1314-9.

Langston C, Kida K, Reed M, Thurlbeck WM. Human lung growth in late gestation and in the neonate. Am Rev Respir Dis. 1984;129:607-13.

Matute-Bello G, Frevert CW, Martin TR. Animal models of acute lung injury. Am J Physiol Lung Cell Mol Physiol. 2008 Sep;295(3):L379-99.

Masood A, Yi M, Lau M, Belcastro R, Shek S, Pan J, Kantores C, McNamara PJ, Kavanagh BP, Belik J, Jankov RP, Tanswell AK. Therapeutic effects of hypercapnia on chronic lung injury and vascular remodeling in neonatal rats. Am J Physiol Lung Cell Mol Physiol. 2009;297:L920-30.

McCurnin DC, Pierce RA, Chang LY, Gibson LL, Osborne-Lawrence S, Yoder BA, Kerecman JD, Albertine KH, Winter VT, Coalson JJ, Crapo JD, Grubb PH, Shaul PW. Inhaled NO improves early pulmonary function and modifies lung growth and elastin deposition in a baboon model of neonatal chronic lung disease. Am J Physiol Lung Cell Mol Physiol. 2005;288:L450-9.

Meinitzer A, Puchinger M, Winklhofer-Roob BM, Rock E, Ribalta J, Roob JM, Sundl I, Halwachs-Baumann G, März W. Reference values for plasma

concentrations of asymmetrical dimethylarginine (ADMA) and other arginine metabolites in men after validation of a chromatographic method. Clin Chim Acta. 2007 Sep;384(1-2):141-8.

Miyake M, Kakimoto Y. Synthesis and degradation of methylated proteins of mouse organs: correlation with protein synthesis and degradation. Metabolism. 1976 Aug;25(8):885-96.

Morris SM Jr. Enzymes of arginine metabolism. J Nutr. 2004 Oct;134(10 Suppl):2743S-7S; discussion 2765S-7S.

Normann E, Lacaze-Masmonteil T, Eaton F, Schwendimann L, Gressens P, and Thebaud B. A novel mouse model of Ureaplasma-induced perinatal inflammation: effects on lung and brain injury. Pediatr Res. 2009;65: 430-6.

Ogawa T, Kimoto M, Sasaoka K. Occurrence of a new enzyme catalyzing the direct conversion of NG,NG-dimethyl-L-arginine to L-citrulline in rats. Biochem Biophys Res Commun. 1987 Oct 29;148(2):671-7.

Ogawa T, Kimoto M, Sasaoka K. Dimethylarginine:pyruvate aminotransferase in rats. Purification, properties, and identity with alanine:glyoxylate aminotransferase 2. J Biol Chem. 1990 Dec 5;265(34):20938-45.

Paik WK, Kim S. Enzymatic methylation of protein fractions from calf thymus nuclei. Biochem Biophys Res Commun. 1967 Oct 11;29(1):14-20.

Piatti PM, Monti LD, Valsecchi G, Magni F, Setola E, Marchesi F, Galli-Kienle M, Pozza G, Alberti KG. Long-term oral L-arginine administration improves peripheral and hepatic insulin sensitivity in type 2 diabetic patients. Diabetes Care. 2001;24:875–80.

Pullamsetti S, Kiss L, Ghofrani HA, Voswinckel R, Haredza P, Klepetko W, Aigner C, Fink L, Muyal JP, Weissmann N, Grimminger F, Seeger W, Schermuly RT. Increased levels and reduced catabolism of asymmetric and symmetric dimethylarginines in pulmonary hypertension. FASEB J. 2005 Jul;19(9):1175-7.

Raetz CR, Ulevitch RJ, Wright SD, Sibley CH, Ding A, Nathan CF. Gram-negative endotoxin: an extraordinary lipid with profound effects on eukaryotic signal transduction. FASEB J. 1991;5:2652–60.

Ryan WL, Wells IC. Homocitrulline and homoarginine synthesis from lysine. Science. 1964;May 29;144(3622):1122-7.

Schromm AB, Brandenburg K, Loppnow H, Moran AP, Koch MH, Rietschel ET, Seydel U. Biological activities of lipopolysaccharides are determined by the shape of their lipid A portion. Eur J Biochem. 2000;267:2008–13.

Schwedhelm E, Maas R, Freese R, Jung D, Lukacs Z, Jambrecina A, Spickler W, Schulze F, Böger RH. Pharmacokinetic and pharmacodynamic properties of oral L-citrulline and L-arginine: impact on nitric oxide metabolism. Br J Clin Pharmacol. 2008;65:51-59.

Schwedhelm E, Maas R, Tan-Andresen J, Schulze F, Riederer U, Böger RH. High-throughput liquid chromatographic-tandem mass spectrometric determination of arginine and dimethylated arginine derivatives in human and mouse plasma. J Chromatogr B Analyt Technol Biomed Life Sci. 2007 May 15;851(1-2):211-9.

Solomonson LP, Flam BR, Pendleton LC, Goodwin BL, Eichler DC. The caveolar nitric oxide synthase/arginine regeneration system for NO production in endothelial cells. J Exp Biol. 2003 Jun;206(Pt 12):2083-7.

Speer CP. Inflammation and bronchopulmonary dysplasia. Semin Neonatol. 2003 Feb;8(1):29-38.

Speer PD, Powers RW, Frank MP, Harger G, Markovic N, Roberts JM. Elevated asymmetric dimethylarginine concentrations precede clinical preeclampsia, but not pregnancies with small-for-gestational-age infants. Am J Obstet Gynecol. 2008 Jan;198(1):112.e1-7.

Sousse LE, Yamamoto Y, Enkhbaatar P, Rehberg SW, Wells SM, Leonard S, Traber MG, Yu YM, Cox RA, Hawkins HK, Traber LD, Herndon DN, Traber DL. Acute lung injury-induced collagen deposition is associated with elevated asymmetric dimethylarginine and arginase activity. Shock. 2011 Mar;35(3):282-8.

ter Horst SA, Walther FJ, Poorthuis BJ, Hiemstra PS, Wagenaar GT (2007) Inhaled nitric oxide attenuates pulmonary inflammation and fibrin deposition and prolongs survival in neonatal hyperoxic lung injury. Am J Physiol Lung Cell Mol Physiol. 2007;293:L35-44.

Thomas W, Seidenspinner S, Kramer BW, Wirbelauer J, Kawczyńska-Leda N, Szymankiewicz M, Speer CP. Airway angiopoietin-2 in ventilated very preterm infants: association with prenatal factors and neonatal outcome. Pediatr Pulmonol. 2011 Aug;46(8):777-84.

Tang JR, Seedorf GJ, Muehlethaler V, Walker DL, Markham NE, Balasubramaniam V, Abman SH. Moderate postnatal hyperoxia accelerates lung growth and attenuates pulmonary hypertension in infant rats after exposure to intra-amniotic endotoxin. Am J Physiol Lung Cell Mol Physiol. 2010;Dec;299(6):L735-48.

Thurlbeck WM. Postnatal growth and development of the lung. Am Rev Respir Dis. 1975;111:803-44.

Tsikas D, Böger RH, Sandmann J, Bode-Böger SM, Frölich JC. Endogenous nitric oxide synthase inhibitors are responsible for the L-arginine paradox. FEBS Lett. 2000 Jul 28;478(1-2):1-3.

Vallance P, Leone A, Calver A, Collier J, Moncada S. Endogenous dimethylarginine as an inhibitor of nitric oxide synthesis. J Cardiovasc Pharmacol. 1992;20 Suppl 12:S60-2.

Velten M, Heyob KM, Rogers LK, and Welty SE. Deficits in lung alveolarization and function after systemic maternal inflammation and neonatal hyperoxia exposure. J Appl Physiol. 2010;108:1347-56.

Walker HA, McGing E, Fisher I, Böger RH, Bode-Böger SM, Jackson G, Ritter JM, Chowienczyk PJ. Endothelium-dependent vasodilation is independent of the plasma L-arginine/ADMA ratio in men with stable angina: lack of effect of oral L-arginine on endothelial function, oxidative stress and exercise performance. J Am Coll Cardiol. 2001;38:499–505.

Watterberg KL, Demers LM, Scott SM, Murphy S. Chorioamnionitis and early lung inflammation in infants in whom bronchopulmonary dysplasia develops. Pediatrics. 1996 Feb;97(2):210-5.

Waugh WH, Daeschner CW 3rd, Files BA, McConnell ME, Strandjord SE. Oral citrulline as arginine precursor may be beneficial in sickle cell disease: early phase two results. J Natl Med Assoc. 2001 Oct;93(10):363-71.

Yi M, Jankov RP, Belcastro R, Humes D, Copland I, Shek S, Sweezey NB, Post M, Albertine KH, Auten RL, Tanswell AK. Opposing effects of 60% oxygen and neutrophil influx on alveologenesis in the neonatal rat. Am J Respir Crit Care Med. 2004;170:1188-96.

Yoon BH, Romero R, Kim KS, Park JS, Ki SH, Kim BI, Jun JK. A systemic fetal inflammatory response and the development of bronchopulmonary dysplasia. Am J Obstet Gynecol. 1999 Oct;181(4):773-9.

Ziche M, Morbidelli L, Choudhuri R, Zhang HT, Donnini S, Granger HJ, Bicknell R (1997) Nitric oxide synthase lies downstream from vascular endothelial growth factor-induced but not basic fibroblast growth factor-induced angiogenesis. J Clin Invest 99:2625-2634

Acknowledgements

My special thanks go to Dr. Patrizia Zaramella and Dr. Giuseppe Giordano.

Many thanks also to Dr. Davide Grisafi whose support was invaluable.

Published Pubmed articles (during the PhD years: 2009/11)

1. Zaglia T, **Dedja A**, Candiotto C, Cozzi E, Schiaffino S, Ausoni S. Cardiac interstitial cells express GATA4 and control dedifferentiation and cell cycle re-entry of adult cardiomyocytes. J Mol Cell Cardiol. 2009 May;46(5):653-62.

2. Villano G, Quarta S, Ruvoletto MG, Turato C, Vidalino L, Biasiolo A, Tono N, Lunardi F, Calabrese F, Dall'Olmo L, **Dedja A**, Fassina G, Gatta A, Pontisso P. Role of squamous cell carcinoma antigen-1 on liver cells after partial hepatectomy in transgenic mice. Int J Mol Med. 2010 Jan;25(1):137-43.

3. Besenzon F, **Dedja A**, Vadori M, Bosio E, Seveso M, Tognato E, Polito L, Calabrese F, Valente M, Rigotti P, Ancona E, Cozzi E. In vitro and in vivo immunomodulatory effects of Cobalt Protoporphyrin administered in combination with immunosuppressive drugs. Transpl Immunol. 2010 Oct;24(1):1-8.

4. Vida VL, **Dedja A**, Faggin E, Speggiorin S, Padalino MA, Boccuzzo G, Pauletto P, Angelini A, Milanesi O, Thiene G, Stellin G. The Effects of Basic Fibroblast Growth Factor in an Animal Model of Acute Mechanically Induced Right Ventricular Hypertrophy. 2012 Jan 27:1-7. [Epub ahead of print].

5. Grisafi D, Tassone E, **Dedja A**, Oselladore B, Masola V, Guzzardo V, Porzionato A, Salmaso R, Albertin G, Artusi C, Zaninotto M, Onisto M, Milan M, Macchi V, De Caro R, Fassina A, Alfiero-Bordigato M, Chiandetti L, Filippone M, Zaramella P. L-citrulline prevents alveolar and vascular derangement in a rat model of moderate hyperoxia-induced lung injury. ***Accepted*** *for publication in: Lung, December 2011*.